Published for SISSA by Springer

Received: April 30, 2012
Accepted: May 24, 2012
Published: June 11, 2012

Dispersive analysis of the scalar form factor of the nucleon

M. Hoferichter,[a] C. Ditsche,[a] B. Kubis[a] and U.-G. Meißner[a,b]

[a] *Helmholtz–Institut für Strahlen- und Kernphysik (Theorie) and Bethe Center for Theoretical Physics, Universität Bonn, D-53115 Bonn, Germany*

[b] *Institut für Kernphysik, Institute for Advanced Simulation and Jülich Center for Hadron Physics, Forschungszentrum Jülich, D-52425 Jülich, Germany*

E-mail: hoferichter@hiskp.uni-bonn.de, ditsche@hiskp.uni-bonn.de, kubis@hiskp.uni-bonn.de, meissner@hiskp.uni-bonn.de

Abstract: Based on the recently proposed Roy-Steiner equations for pion-nucleon (πN) scattering [1], we derive a system of coupled integral equations for the $\pi\pi \to \bar{N}N$ and $\bar{K}K \to \bar{N}N$ S-waves. These equations take the form of a two-channel Muskhelishvili-Omnès problem, whose solution in the presence of a finite matching point is discussed. We use these results to update the dispersive analysis of the scalar form factor of the nucleon fully including $\bar{K}K$ intermediate states. In particular, we determine the correction $\Delta_\sigma = \sigma(2M_\pi^2) - \sigma_{\pi N}$, which is needed for the extraction of the pion-nucleon σ term from πN scattering, as a function of pion-nucleon subthreshold parameters and the πN coupling constant.

Keywords: Chiral Lagrangians, QCD

ArXiv ePrint: 1204.6251

doi:10.1007/JHEP06(2012)063

JHEP06(2012)063

Contents

1 Introduction

The standard procedure to extract the pion-nucleon σ term $\sigma_{\pi N}$, the nucleon form factor $\sigma(t)$ of the scalar current $\hat{m}(\bar{u}u + \bar{d}d)$ at vanishing momentum transfer $t = 0$ (here $\hat{m} = (m_{\mathrm{u}} + m_{\mathrm{d}})/2$ denotes the average mass of the light quarks), from πN scattering data involves the venerable low-energy theorem that relates the Born-term-subtracted isoscalar πN scattering amplitude at the Cheng-Dashen point to $\sigma(2M_\pi^2)$ [2, 3]. Later on, it was shown that the corrections to this low-energy theorem are very small, in particular they are free of chiral logarithms at full one-loop order in chiral perturbation theory (ChPT) [4, 5]. The extraction of $\sigma_{\pi N}$ itself thus requires knowledge of the difference

$$\Delta_\sigma = \sigma(2M_\pi^2) - \sigma_{\pi N} \,, \tag{1.1}$$

which can be determined by means of a dispersive representation of $\sigma(t)$ [6]. The leading contribution to the imaginary part originates from $\pi\pi$ intermediate states, so that, upon neglecting higher terms in the spectral function, $\operatorname{Im}\sigma(t)$ can be expressed in terms of the scalar pion form factor $F_\pi^S(t)$ and the $\pi\pi \to \bar{N}N$ S-wave $f_+^0(t)$. Relying on the results of [7] for $F_\pi^S(t)$ and of [8] for $f_+^0(t)$ led to the estimate [6]

$$\Delta_\sigma = (15.2 \pm 0.4)\,\text{MeV}\,, \tag{1.2}$$

where the error only includes the uncertainty in the parameterization of the $\pi\pi$ phase available at that time. In particular, one should note that the contributions from $\bar{K}K$ intermediate states in the determination of $f_+^0(t)$ and the unitarity relation for $\sigma(t)$ were neglected, while being included in the calculation of $F_\pi^S(t)$. Although the dominant effect may indeed be expected in the pion form factor, such a treatment is strictly speaking inconsistent and leads to an additional uncertainty in (1.2) that is difficult to quantify. Moreover, the result for $f_+^0(t)$ from [8] corresponds to particular values of πN subthreshold parameters and the πN coupling constant. Especially the value $g^2/4\pi = 14.28$ used for the coupling constant cannot be reconciled with more recent determinations [9–12].

In this article we perform an updated dispersive analysis of the scalar form factor of the nucleon. Based on Roy-Steiner (RS) equations for pion-nucleon scattering [1], we determine the $\pi\pi \to \bar{N}N$ and $\bar{K}K \to \bar{N}N$ S-waves as solutions of a two-channel Muskhelishvili-Omnès (MO) problem and repeat the calculation of the scalar pion and kaon form factors for our input of $\pi\pi$ and $\pi\pi \to \bar{K}K$ partial waves. Taking everything together, we then analyze the spectral function of the scalar form factor of the nucleon fully including the effects from $\bar{K}K$ intermediate states, and provide an updated value for Δ_σ as a function of πN subthreshold parameters and the πN coupling constant.

The paper is organized as follows. In section 2 we consider a generic two-channel MO problem with finite matching point and develop a method to construct the corresponding Omnès matrix, which we apply to the coupled system of $\pi\pi \to \bar{N}N$ and $\bar{K}K \to \bar{N}N$ S-waves in section 3. In section 4 we first present our results for the scalar pion and kaon form factors, which are then used as input for the dispersive analysis of the scalar form factor of the nucleon. We offer our conclusions in section 5. Several technical details of the calculation are relegated to the appendices.

2 Two-channel Muskhelishvili-Omnès problem

We consider the generic coupled-channel integral equation

$$\mathbf{f}(t) = \mathbf{\Delta}(t) + \frac{1}{\pi}\int\limits_{t_\pi}^{t_\mathrm{m}} \mathrm{d}t' \frac{T^*(t')\Sigma(t')\mathbf{f}(t')}{t'-t} + \frac{1}{\pi}\int\limits_{t_\mathrm{m}}^{\infty} \mathrm{d}t' \frac{\mathrm{Im}\,\mathbf{f}(t')}{t'-t}\,, \tag{2.1}$$

where bold-faced quantities are two-dimensional vectors in channel space, representing pion and kaon intermediate states,[1] and the imaginary part of $\mathbf{f}(t)$ is assumed to be known above the matching point t_m. In particular, $f_1(t)$ and $f_2(t)$ can be thought of as the $\pi\pi \to \bar{N}N$ and $\bar{K}K \to \bar{N}N$ S-waves, respectively, although the following discussion can be carried

[1]Throughout this work, we neglect 4π intermediate states, which are phenomenologically irrelevant at low energies. In fact, the effective onset of 4π inelasticities marks the breakdown of the present two-channel model, cf. section 3.

JHEP06(2012)063

out for general angular momentum J. The function $\mathbf{\Delta}(t)$ contains at most left-hand cuts and is therefore real for $t \geq t_\pi = 4M_\pi^2$. The unitarity relation is written in the form

$$\operatorname{Im} \mathbf{f}(t) = T^*(t)\Sigma(t)\mathbf{f}(t) \; , \tag{2.2}$$

with T-matrix $T(t)$ and phase-space factor $\Sigma(t)$ parameterized as[2]

$$T(t) = \begin{pmatrix} \frac{\eta(t)e^{2i\delta(t)}-1}{2i\sigma_t^\pi q_t^{2J}} & |g(t)|e^{i\psi(t)} \\ |g(t)|e^{i\psi(t)} & \frac{\eta(t)e^{2i(\psi(t)-\delta(t))}-1}{2i\sigma_t^K k_t^{2J}} \end{pmatrix} , \quad \Sigma(t) = \operatorname{diag}\Big(\sigma_t^\pi q_t^{2J}\theta\big(t-t_\pi\big), \sigma_t^K k_t^{2J}\theta\big(t-t_K\big)\Big), \tag{2.3}$$

with pion, kaon, and — for later use — nucleon t-channel momenta

$$q_t = \sqrt{\frac{t}{4} - M_\pi^2} = \frac{\sqrt{t}}{2}\sigma_t^\pi \; , \quad k_t = \sqrt{\frac{t}{4} - M_K^2} = \frac{\sqrt{t}}{2}\sigma_t^K \; , \quad p_t = \sqrt{\frac{t}{4} - m^2} = \frac{\sqrt{t}}{2}\sigma_t^N \; , \tag{2.4}$$

and the two-kaon threshold $t_K = 4M_K^2$. The scattering phases $\delta(t)$ and $\psi(t)$ are required as input for $t_\pi \leq t \leq t_\mathrm{m}$, where Watson's theorem [14] demands $\psi(t) = \delta(t)$ for $t \leq t_K$. Moreover, the modulus of the $\pi\pi \to \bar{K}K$ S-wave $g(t)$ is needed in the full range $t_\pi \leq t \leq t_\mathrm{m}$, and thus has to be analytically continued into the pseudophysical region $t_\pi \leq t \leq t_K$. Finally, the inleasticity parameter $\eta(t)$ can be related to $|g(t)|$ via

$$\eta(t) = \sqrt{1 - 4\sigma_t^\pi \sigma_t^K (q_t k_t)^{2J} |g(t)|^2 \theta\big(t - t_K\big)} \; , \tag{2.5}$$

and the relation between S- and T-matrix reads

$$S(t) = \mathbb{1} + 2i\, \Sigma^{1/2}(t)T(t)\Sigma^{1/2}(t) \; . \tag{2.6}$$

2.1 Formal solution

We define the Omnès matrix $\Omega(t)$ by

$$\begin{Bmatrix} \operatorname{Im}\Omega(t) = T^*(t)\Sigma(t)\Omega(t) \\ \operatorname{Im}\Omega(t) = 0 \end{Bmatrix} \quad \text{for} \quad \begin{Bmatrix} t_\pi \leq t \leq t_\mathrm{m} \\ \text{otherwise} \end{Bmatrix} \tag{2.7}$$

and choose the normalization $\Omega(0) = \mathbb{1}$. Writing

$$\mathbf{F}(t) = \mathbf{f}(t) - \mathbf{\Delta}(t) = \Omega(t)\mathbf{G}(t) \; , \tag{2.8}$$

it follows that for $t \geq t_\pi$

$$\big(\mathbb{1} - 2i\, T^*(t)\Sigma(t)\big)\Omega(t_+)\big(\mathbf{G}(t_+) - \mathbf{G}(t_-)\big) = 2i\, T^*(t)\Sigma(t)\mathbf{\Delta}(t) \; , \tag{2.9}$$

where $t_\pm = t \pm i\epsilon$ and the physical limit is given by t_+. Using unitarity in the form

$$\big(\mathbb{1} - 2i\, T^*(t)\Sigma(t)\big)^{-1} = \mathbb{1} + 2i\, T(t)\Sigma(t) \; , \tag{2.10}$$

[2] The masses of nucleon, pion, and kaon are denoted by m, M_π, and M_K, respectively, and defined by the charged-particle masses as given in [13].

JHEP06(2012)063

which in particular holds for $t \le t_K$ by virtue of Watson's theorem, we find

$$\mathbf{G}(t_+) - \mathbf{G}(t_-) = 2i\,\Omega^{-1}(t)T(t)\Sigma(t)\boldsymbol{\Delta}(t)\,, \tag{2.11}$$

and thus

$$\begin{aligned}\mathbf{f}(t) &= \boldsymbol{\Delta}(t) + \frac{\Omega(t)}{\pi}\int_{t_\pi}^{t_\mathrm{m}} \mathrm{d}t' \frac{\Omega^{-1}(t')T(t')\Sigma(t')\boldsymbol{\Delta}(t')}{t'-t} + \frac{\Omega(t)}{\pi}\int_{t_\mathrm{m}}^{\infty} \mathrm{d}t' \frac{\Omega^{-1}(t')\mathrm{Im}\,\mathbf{f}(t')}{t'-t} \\ &= \boldsymbol{\Delta}(t) - \frac{\Omega(t)}{\pi}\int_{t_\pi}^{t_\mathrm{m}} \mathrm{d}t' \frac{\mathrm{Im}\,\Omega^{-1}(t')\boldsymbol{\Delta}(t')}{t'-t} + \frac{\Omega(t)}{\pi}\int_{t_\mathrm{m}}^{\infty} \mathrm{d}t' \frac{\Omega^{-1}(t')\mathrm{Im}\,\mathbf{f}(t')}{t'-t}\,. \end{aligned} \tag{2.12}$$

The problem is such reduced to finding a matrix $\Omega(t)$ that fulfills (2.7). For $t_\pi \le t \le t_K$ we have

$$\Omega(t_+) = \big(\mathbb{1} + 2i\,T(t)\Sigma(t)\big)\Omega(t_-)\,. \tag{2.13}$$

Taking the determinant on both sides yields, again using Watson's theorem for $t \le t_K$,

$$\det\Omega(t_+) = e^{2i\psi(t)}\det\Omega(t_-)\,, \tag{2.14}$$

and thus [15]

$$\det\Omega(t) = \exp\left\{\frac{t}{\pi}\int_{t_\pi}^{t_\mathrm{m}} \mathrm{d}t' \frac{\psi(t')}{t'(t'-t)}\right\}. \tag{2.15}$$

Although the determinant allows for an analytic solution in the same way as in the single-channel case [16], there is in general no analytic solution for the Omnès matrix itself even for an infinite matching point, which therefore has to be calculated numerically, either by an iterative procedure [7] or a discretization method, i.e. solving a matrix equation [15, 17] (for a mathematician's point of view see [18]). Similarly to the single-channel case, we expect a cusp at t_m, which has to be taken into account in the numerical evaluation of the integrals in (2.12) (see [1, 19]). Indeed, for $t \to t_\mathrm{m}$ the determinant behaves as

$$\det\Omega(t) \sim |t_\mathrm{m} - t|^x\,, \qquad x = \frac{\psi(t_\mathrm{m})}{\pi}\,. \tag{2.16}$$

Accordingly, we write for $t \to t_\mathrm{m}$ from below

$$\det\Omega(t) = \det\bar\Omega(t_\mathrm{m})e^{i\pi x}|t_\mathrm{m} - t|^x\,, \qquad \Omega_{ij}(t) = \bar\Omega_{ij}(t_\mathrm{m})e^{i\delta_{ij}(t_\mathrm{m})}|t_\mathrm{m} - t|^{x_{ij}}\,, \tag{2.17}$$

and from above

$$\det\Omega(t) = \det\bar\Omega(t_\mathrm{m})|t_\mathrm{m} - t|^x\,, \qquad \Omega_{ij}(t) = \bar\Omega_{ij}(t_\mathrm{m})|t_\mathrm{m} - t|^{x_{ij}}\,, \tag{2.18}$$

since $\Omega(t)$ is real above t_m. Here, we have assumed that the (real) functions $\bar\Omega_{ij}(t)$ are continuous at t_m. The strength of the cusp in each component $\Omega_{ij}(t)$ of the Omnès matrix is determined by the numbers x_{ij}, whose relation to the S-matrix parameters will be established in the following sections. Throughout this paper we will consider the case $0 < x_{ij} < 1$, which is relevant for the coupled-channel S-wave system of $\pi\pi$ and $\bar KK$ intermediate states. The extension to arbitrary values of x_{ij} can then be done along the lines described in [19, 20].

JHEP06(2012)063

2.2 Dispersive representation of the Omnès matrix

For $0 < x_{ij} < 1$ we may write down a dispersive representation

$$\Omega(t) = \left(1 - \frac{t}{t_{\mathrm{m}}}\right)\mathbb{1} + \frac{t(t-t_{\mathrm{m}})}{\pi} \int_{t_\pi}^{t_{\mathrm{m}}} \mathrm{d}t' \, \frac{T^*(t')\Sigma(t')\Omega(t')}{t'(t'-t_{\mathrm{m}})(t'-t)} \,, \tag{2.19}$$

where the subtraction constants have been fixed in such a way that $\Omega(0) = \mathbb{1}$ and $\Omega(t_{\mathrm{m}}) = 0$. In particular, we can investigate the limit $t \to t_{\mathrm{m}}$ to obtain information on x_{ij}. Using the asymptotic form of the integrals [19] (the dash denotes the principal-value part of the integral)

$$\begin{aligned}
\frac{|t_{\mathrm{m}} - t|^x}{\pi} \fint_{t_{\mathrm{m}}-\epsilon}^{t_{\mathrm{m}}} \frac{\mathrm{d}t'}{(t'-t)|t_{\mathrm{m}} - t'|^x} &\xrightarrow{\epsilon \to 0,\, t \to t_{\mathrm{m}}} \frac{1}{\pi} \fint_0^\infty \frac{\mathrm{d}v}{v^x(1-v)} = -\cot \pi x \,, \\
\frac{|t_{\mathrm{m}} - t|^x}{\pi} \int_{t_{\mathrm{m}}}^{t_{\mathrm{m}}+\epsilon} \frac{\mathrm{d}t'}{(t'-t)|t_{\mathrm{m}} - t'|^x} &\xrightarrow{\epsilon \to 0,\, t \to t_{\mathrm{m}}} \frac{1}{\pi} \int_0^\infty \frac{\mathrm{d}v}{v^x(1+v)} = \frac{1}{\sin \pi x} \,,
\end{aligned} \tag{2.20}$$

we obtain for $t \to t_{\mathrm{m}}$ from below[3]

$$\begin{aligned}
\bar\Omega_{11}|t_{\mathrm{m}} - t|^{x_{11}} e^{i\delta_{11}} &= \bar\Omega_{11}|t_{\mathrm{m}} - t|^{x_{11}} e^{i\delta_{11}} \frac{e^{i\pi x_{11}}}{\sin \pi x_{11}} \frac{1 - \eta e^{-2i\delta}}{2i} \\
&\quad + \bar\Omega_{21}|t_{\mathrm{m}} - t|^{x_{21}} e^{i\delta_{21}} \frac{e^{i\pi x_{21}}}{\sin \pi x_{21}} |g| \sigma^K_{t_{\mathrm{m}}} e^{-i\psi} \,, \\
\bar\Omega_{12}|t_{\mathrm{m}} - t|^{x_{12}} e^{i\delta_{12}} &= \bar\Omega_{12}|t_{\mathrm{m}} - t|^{x_{12}} e^{i\delta_{12}} \frac{e^{i\pi x_{12}}}{\sin \pi x_{12}} \frac{1 - \eta e^{-2i\delta}}{2i} \\
&\quad + \bar\Omega_{22}|t_{\mathrm{m}} - t|^{x_{22}} e^{i\delta_{22}} \frac{e^{i\pi x_{22}}}{\sin \pi x_{22}} |g| \sigma^K_{t_{\mathrm{m}}} e^{-i\psi} \,, \\
\bar\Omega_{21}|t_{\mathrm{m}} - t|^{x_{21}} e^{i\delta_{21}} &= \bar\Omega_{11}|t_{\mathrm{m}} - t|^{x_{11}} e^{i\delta_{11}} \frac{e^{i\pi x_{11}}}{\sin \pi x_{11}} |g| \sigma^\pi_{t_{\mathrm{m}}} e^{-i\psi} \\
&\quad + \bar\Omega_{21}|t_{\mathrm{m}} - t|^{x_{21}} e^{i\delta_{21}} \frac{e^{i\pi x_{21}}}{\sin \pi x_{21}} \frac{1 - \eta e^{-2i(\psi-\delta)}}{2i} \,, \\
\bar\Omega_{22}|t_{\mathrm{m}} - t|^{x_{22}} e^{i\delta_{22}} &= \bar\Omega_{12}|t_{\mathrm{m}} - t|^{x_{12}} e^{i\delta_{12}} \frac{e^{i\pi x_{12}}}{\sin \pi x_{12}} |g| \sigma^\pi_{t_{\mathrm{m}}} e^{-i\psi} \\
&\quad + \bar\Omega_{22}|t_{\mathrm{m}} - t|^{x_{22}} e^{i\delta_{22}} \frac{e^{i\pi x_{22}}}{\sin \pi x_{22}} \frac{1 - \eta e^{-2i(\psi-\delta)}}{2i} \,,
\end{aligned} \tag{2.21}$$

and for $t \to t_{\mathrm{m}}$ from above

$$\begin{aligned}
\bar\Omega_{11}|t_{\mathrm{m}} - t|^{x_{11}} &= \bar\Omega_{11}|t_{\mathrm{m}} - t|^{x_{11}} \frac{e^{i\delta_{11}}}{\sin \pi x_{11}} \frac{1 - \eta e^{-2i\delta}}{2i} + \bar\Omega_{21}|t_{\mathrm{m}} - t|^{x_{21}} \frac{e^{i\delta_{21}}}{\sin \pi x_{21}} |g| \sigma^K_{t_{\mathrm{m}}} e^{-i\psi} \,, \\
\bar\Omega_{12}|t_{\mathrm{m}} - t|^{x_{12}} &= \bar\Omega_{12}|t_{\mathrm{m}} - t|^{x_{12}} \frac{e^{i\delta_{12}}}{\sin \pi x_{12}} \frac{1 - \eta e^{-2i\delta}}{2i} + \bar\Omega_{22}|t_{\mathrm{m}} - t|^{x_{22}} \frac{e^{i\delta_{22}}}{\sin \pi x_{22}} |g| \sigma^K_{t_{\mathrm{m}}} e^{-i\psi} \,,
\end{aligned}$$

[3] We consider the case $J = 0$ for simplicity. The general case can always be recovered by introducing the correct phase-space factors according to $\sigma^\pi_t \to \sigma^\pi_t q_t^{2J}$ and $\sigma^K_t \to \sigma^K_t k_t^{2J}$.

JHEP06(2012)063

$$
\begin{aligned}
\bar\Omega_{21}|t_{\rm m}-t|^{x_{21}} &= \bar\Omega_{11}|t_{\rm m}-t|^{x_{11}}\frac{e^{i\delta_{11}}}{\sin\pi x_{11}}|g|\sigma^{\pi}_{t_{\rm m}}e^{-i\psi}+\bar\Omega_{21}|t_{\rm m}-t|^{x_{21}}\frac{e^{i\delta_{21}}}{\sin\pi x_{21}}\frac{1-\eta e^{-2i(\psi-\delta)}}{2i}\,,\\
\bar\Omega_{22}|t_{\rm m}-t|^{x_{22}} &= \bar\Omega_{12}|t_{\rm m}-t|^{x_{12}}\frac{e^{i\delta_{12}}}{\sin\pi x_{12}}|g|\sigma^{\pi}_{t_{\rm m}}e^{-i\psi}+\bar\Omega_{22}|t_{\rm m}-t|^{x_{22}}\frac{e^{i\delta_{22}}}{\sin\pi x_{22}}\frac{1-\eta e^{-2i(\psi-\delta)}}{2i}\,,
\end{aligned}
\tag{2.22}
$$

where we have suppressed the evaluation at $t_{\rm m}$ wherever possible. If we assume that $g(t_{\rm m})\neq 0$ and $\bar\Omega_{ij}(t_{\rm m})\neq 0$ (which can always be achieved by choosing the matching point appropriately), we can conclude from the first line of (2.21) that $x_{21}\geq x_{11}$, since otherwise g or $\bar\Omega_{21}$ would have to vanish at $t_{\rm m}$. Conversely, the third line requires $x_{21}\leq x_{11}$ by the same argument, and hence $x_{11}=x_{21}$. Similarly, we find $x_{12}=x_{22}$. Moreover, as the determinant behaves according to (2.16), we can conclude that $x_{11}+x_{12}=x$, again provided that $\det\bar\Omega(t_{\rm m})\neq 0$. Dividing the first line of (2.21) by the first line of (2.22), we find

$$
e^{i\delta_{11}}\left(1-\frac{e^{i\pi x_{11}}}{\sin\pi x_{11}}\frac{1-\eta e^{-2i\delta}}{2i}\right)=e^{i\pi x_{21}}\left(1-\frac{e^{i\delta_{11}}}{\sin\pi x_{11}}\frac{1-\eta e^{-2i\delta}}{2i}\right)\,, \tag{2.23}
$$

which for $x_{21}=x_{11}$ reduces to

$$
e^{i\delta_{11}}=e^{i\pi x_{11}}\,, \tag{2.24}
$$

and thus $\pi x_{11}=\delta_{11}$ up to integer multiples of 2π. Arguing analogously for x_{12}, these results can be summarized as

$$
x_{11}=x_{21}\,,\qquad x_{12}=x_{22}\,,\qquad x_{ij}=\frac{\delta_{ij}}{\pi}\,,\qquad x_{11}+x_{12}=x\,. \tag{2.25}
$$

By virtue of (2.25), (2.21) and (2.22) take the form

$$
\begin{aligned}
&\begin{pmatrix}\frac{e^{i\pi x_{11}}}{\sin\pi x_{11}}\frac{1-\eta e^{-2i\delta}}{2i}-1 & \frac{e^{i\pi x_{11}}}{\sin\pi x_{11}}|g|\sigma^{K}_{t_{\rm m}}e^{-i\psi}\\ \frac{e^{i\pi x_{11}}}{\sin\pi x_{11}}|g|\sigma^{\pi}_{t_{\rm m}}e^{-i\psi} & \frac{e^{i\pi x_{11}}}{\sin\pi x_{11}}\frac{1-\eta e^{-2i(\psi-\delta)}}{2i}-1\end{pmatrix}\begin{pmatrix}\bar\Omega_{11}\\ \bar\Omega_{21}\end{pmatrix}=0\,,\\
&\begin{pmatrix}\frac{e^{i\pi x_{12}}}{\sin\pi x_{12}}\frac{1-\eta e^{-2i\delta}}{2i}-1 & \frac{e^{i\pi x_{12}}}{\sin\pi x_{12}}|g|\sigma^{K}_{t_{\rm m}}e^{-i\psi}\\ \frac{e^{i\pi x_{12}}}{\sin\pi x_{12}}|g|\sigma^{\pi}_{t_{\rm m}}e^{-i\psi} & \frac{e^{i\pi x_{12}}}{\sin\pi x_{12}}\frac{1-\eta e^{-2i(\psi-\delta)}}{2i}-1\end{pmatrix}\begin{pmatrix}\bar\Omega_{12}\\ \bar\Omega_{22}\end{pmatrix}=0\,.
\end{aligned}
\tag{2.26}
$$

To ensure the existence of non-trivial solutions the determinants of the coefficient matrices must vanish. This leads to

$$
\cos\pi(2x_{11}-x)-\eta\cos\pi(2y-x)=0\,,\quad \cos\pi(2x_{12}-x)-\eta\cos\pi(2y-x)=0\,,\quad y=\frac{\delta(t_{\rm m})}{\pi}\,. \tag{2.27}
$$

These conditions are invariant under $x_{11}\to x-x_{11}$, i.e. there is an ambiguity between x_{11} and x_{12}. However, demanding that x_{11} coincide with x in the single-channel limit yields

$$
x_{11}=\frac{1}{2}\Big\{x+\frac{1}{\pi}\arccos(\eta\cos\pi(2y-x))\Big\}\,,\quad x_{12}=\frac{1}{2}\Big\{x-\frac{1}{\pi}\arccos(\eta\cos\pi(2y-x))\Big\}\,. \tag{2.28}
$$

JHEP06(2012)063

Finally, (2.26) together with (2.28) and

$$\begin{aligned}
&\sin\pi x_{11} = \sin\frac{\pi x}{2}\sqrt{\frac{1+z}{2}} + \cos\frac{\pi x}{2}\sqrt{\frac{1-z}{2}}\,, \qquad \cos\pi x_{11} = \cos\frac{\pi x}{2}\sqrt{\frac{1+z}{2}} - \sin\frac{\pi x}{2}\sqrt{\frac{1-z}{2}}\,, \\
&\sin\pi x_{12} = \sin\frac{\pi x}{2}\sqrt{\frac{1+z}{2}} - \cos\frac{\pi x}{2}\sqrt{\frac{1-z}{2}}\,, \qquad \cos\pi x_{12} = \cos\frac{\pi x}{2}\sqrt{\frac{1+z}{2}} + \sin\frac{\pi x}{2}\sqrt{\frac{1-z}{2}}\,, \\
&\qquad z = \eta\cos\pi(2y-x)\,,
\end{aligned} \tag{2.29}$$

can be used to derive constraints on $\bar{\Omega}_{ij}$. We find

$$\frac{\bar{\Omega}_{21}}{\bar{\Omega}_{11}} = \frac{N}{2|g|\sigma^K_{t_\mathrm{m}}}\,, \qquad \frac{\bar{\Omega}_{12}}{\bar{\Omega}_{22}} = -\frac{N}{2|g|\sigma^\pi_{t_\mathrm{m}}}\,, \qquad N = \sqrt{1-\eta^2\cos^2\pi(2y-x)} - \eta\sin\pi(2y-x)\,. \tag{2.30}$$

In the single-channel case one can show that, using the integrals (2.20), the solution for $f(t)$ is automatically continuous at t_m [19]. In fact, the same statement holds true also in the two-channel case. The relations (2.30) are essential in the proof, as demonstrated in appendix A.

2.3 Construction of the Omnès matrix

2.3.1 Infinite matching point

Our construction of the two-channel Omnès matrix with finite matching point will heavily rely on the solution for its infinite-matching-point analog $\Omega^\infty(t)$, whose defining property can be stated as

$$\begin{Bmatrix} \mathrm{Im}\,\Omega^\infty(t) = T^*(t)\Sigma(t)\Omega^\infty(t) \\ \mathrm{Im}\,\Omega^\infty(t) = 0 \end{Bmatrix} \quad \text{for} \quad \begin{Bmatrix} t \geq t_\pi \\ \text{otherwise} \end{Bmatrix}\,. \tag{2.31}$$

For its calculation we follow [15] and discretize the unsubtracted dispersion relation

$$\mathrm{Re}\,\Omega^\infty(t) = \frac{1}{\pi}\,\fint_{t_\pi}^{\infty} \mathrm{d}t'\,\frac{\mathrm{Im}\,\Omega^\infty(t')}{t'-t} \tag{2.32}$$

on a set of Gauß-Legendre integration points. Note that an unsubtracted dispersion relation converges provided that the phase-shift at infinity is positive. In the one-channel case this can be directly deduced from the explicit solution

$$\Omega^\infty(t) = \exp\left\{\frac{t}{\pi}\int_{t_\pi}^{\infty}\mathrm{d}t'\,\frac{\delta(t')}{t'(t'-t)}\right\}, \tag{2.33}$$

which behaves as

$$\Omega^\infty(t) \sim t^{-\frac{\delta(\infty)}{\pi}} \tag{2.34}$$

for large t. The unitarity condition (2.31) can be rewritten as

$$\mathrm{Im}\,\mathbf{\Omega}^\infty_i = \begin{pmatrix} \frac{\eta\sin(2\delta-\psi)+\sin\psi}{\eta\cos(2\delta-\psi)+\cos\psi} & \frac{2|g|\sigma^K_t\theta(t-t_K)}{\eta\cos(2\delta-\psi)+\cos\psi} \\ \frac{2|g|\sigma^\pi_t}{\eta\cos(2\delta-\psi)+\cos\psi} & -\frac{\eta\sin(2\delta-\psi)-\sin\psi}{\eta\cos(2\delta-\psi)+\cos\psi} \end{pmatrix} \mathrm{Re}\,\mathbf{\Omega}^\infty_i\,, \qquad i\in\{1,2\}\,, \tag{2.35}$$

with

$$\mathbf{\Omega}_1^\infty = \begin{pmatrix} \Omega_{11}^\infty \\ \Omega_{21}^\infty \end{pmatrix} , \qquad \mathbf{\Omega}_2^\infty = \begin{pmatrix} \Omega_{12}^\infty \\ \Omega_{22}^\infty \end{pmatrix} , \tag{2.36}$$

which below the two-kaon threshold reduces to

$$\operatorname{Im} \mathbf{\Omega}_i^\infty = \begin{pmatrix} \tan\delta & 0 \\ \frac{|g|\sigma_t^\pi}{\cos\delta} & 0 \end{pmatrix} \operatorname{Re} \mathbf{\Omega}_i^\infty . \tag{2.37}$$

The details of the numerical solution of the corresponding integral equation for $\operatorname{Re} \mathbf{\Omega}_i^\infty$ are described in [15, 17].

2.3.2 Finite matching point, single-channel case

An Omnès function with a finite matching point does not allow for an unsubtracted dispersion relation, since the solution (2.15) tends to a constant for $t \to \infty$, and consequently one picks up contributions at infinity. Moreover, the cusp at the matching point renders both the discretization method and an iterative procedure involving subtracted dispersion relations inappropriate, as neither is able to accurately reproduce the analytic behavior around t_m. For this reason, the aim of this section is to establish a method that relies on the known solution in the infinite-matching-point scenario.

We first observe that the function

$$\xi(t) = \left(\frac{t_\mathrm{m} - t}{t_\mathrm{m}}\right)^{x(t)} = \left|\frac{t_\mathrm{m} - t}{t_\mathrm{m}}\right|^{x(t)} e^{-i\pi x(t)\theta(t-t_\mathrm{m})} \tag{2.38}$$

has the correct properties to cancel an imaginary part above t_m. Indeed, the function

$$\Omega(t) = \Omega^\infty(t)\xi(t) , \tag{2.39}$$

with $\Omega^\infty(t)$ from (2.33), fulfills

$$\left\{ \begin{matrix} \operatorname{Im}\Omega(t) = T^*(t)\Sigma(t)\Omega(t) \\ \operatorname{Im}\Omega(t) = \Omega^\infty(t)|\xi(t)|\Big(e^{i(\pi x(t)-\delta(t))}\sin\delta(t) - \sin\pi x(t)\Big) \end{matrix} \right\} \quad \text{for} \quad \left\{ \begin{matrix} t_\pi \leq t \leq t_\mathrm{m} \\ t \geq t_\mathrm{m} \end{matrix} \right\}, \tag{2.40}$$

and with the choice

$$\left\{ \begin{matrix} x(t) = \frac{\delta(t_\mathrm{m})}{\pi} \\ x(t) = \frac{\delta(t)}{\pi} \end{matrix} \right\} \quad \text{for} \quad \left\{ \begin{matrix} t \leq t_\mathrm{m} \\ t \geq t_\mathrm{m} \end{matrix} \right\} \tag{2.41}$$

the defining property (2.7) holds. Since we know the analytic solution, we can study the properties of this construction in more detail

$$\Omega(t) = \exp\left\{ \frac{t}{\pi} \int_{t_\pi}^{t_\mathrm{m}} \mathrm{d}t' \frac{\delta(t')}{t'(t'-t)} \right\} \exp\left\{ \frac{t}{\pi} \int_{t_\mathrm{m}}^{\infty} \mathrm{d}t' \frac{\delta(t') - \pi x(t)}{t'(t'-t)} \right\} . \tag{2.42}$$

The first term coincides with the expected result for the single-channel case, while the second factor is new. It is indeed real, and thus preserves all defining properties, in particular the normalization $\Omega(0) = 1$. This example shows that we would exactly recover the result (2.15) if we did not know the solution for a finite matching point, constructed it according to (2.39), and chose $\delta(t) = \delta(t_\mathrm{m})$ for t above the matching point. Obviously, (2.42) implies that “the” Omnès function is not unique. The derivation of (2.12), however, only relies on the defining properties and is therefore independent of such modifications.

JHEP06(2012)063

2.3.3 Finite matching point, two-channel case

To generalize the preceding considerations to the two-channel case we define a matrix

$$\xi_{ij}(t) = \bar{\xi}_{ij}(t)\left(\frac{t_{\rm m}-t}{t_{\rm m}}\right)^{x_{ij}(t)} \tag{2.43}$$

with real functions $\bar{\xi}_{ij}(t)$. In view of the results of the previous section we take phases and inelasticities constant above $t_{\rm m}$ and thus can ignore the t-dependence of x_{ij} and $\bar{\xi}_{ij}$, which in the following will always be understood to be evaluated at $t_{\rm m}$. It is straightforward to show that

$$\begin{Bmatrix} \Omega(t) = a(t)\Omega^{\infty}(t)\xi(t) \\ \Omega(t) = a(t)(\Omega^{\infty})^T(t)\xi(t) \end{Bmatrix} \quad \text{for} \quad \begin{Bmatrix} t \le t_{\rm m} \\ t \ge t_{\rm m} \end{Bmatrix} , \tag{2.44}$$

with infinite-matching-point solution $\Omega^{\infty}(t)$ and a real matrix $a(t)$, fulfills (2.7) provided that

$$\begin{aligned} \operatorname{Im}\xi^T(t) + \xi^T(t)T(t)\Sigma(t) &= 0 \qquad \text{for } t \ge t_{\rm m} \,, \\ \big[a(t), T^*(t)\Sigma(t)\big] &= 0 \qquad \text{for } t \le t_{\rm m} \,. \end{aligned} \tag{2.45}$$

Imposing $x_{11} = x_{21} = x - x_{12} = x - x_{22}$, the first condition corresponds to

$$\begin{aligned} &\begin{pmatrix} \frac{e^{i\pi x_{11}}}{\sin\pi x_{11}}\frac{1-\eta e^{-2i\delta}}{2i} - 1 & \frac{e^{i\pi x_{11}}}{\sin\pi x_{11}}|g|\sigma^{\pi}_{t_{\rm m}}e^{-i\psi} \\ \frac{e^{i\pi x_{11}}}{\sin\pi x_{11}}|g|\sigma^{K}_{t_{\rm m}}e^{-i\psi} & \frac{e^{i\pi x_{11}}}{\sin\pi x_{11}}\frac{1-\eta e^{-2i(\psi-\delta)}}{2i} - 1 \end{pmatrix}\begin{pmatrix} \bar{\xi}_{11} \\ \bar{\xi}_{21} \end{pmatrix} = 0 \,, \\ &\begin{pmatrix} \frac{e^{i\pi x_{12}}}{\sin\pi x_{12}}\frac{1-\eta e^{-2i\delta}}{2i} - 1 & \frac{e^{i\pi x_{12}}}{\sin\pi x_{12}}|g|\sigma^{\pi}_{t_{\rm m}}e^{-i\psi} \\ \frac{e^{i\pi x_{12}}}{\sin\pi x_{12}}|g|\sigma^{K}_{t_{\rm m}}e^{-i\psi} & \frac{e^{i\pi x_{12}}}{\sin\pi x_{12}}\frac{1-\eta e^{-2i(\psi-\delta)}}{2i} - 1 \end{pmatrix}\begin{pmatrix} \bar{\xi}_{12} \\ \bar{\xi}_{22} \end{pmatrix} = 0 \,. \end{aligned} \tag{2.46}$$

Non-trivial solutions of (2.46) again exist for x_{11} and x_{12} given by (2.28), while the components of $\xi(t)$ are related by

$$\frac{\bar{\xi}_{21}}{\bar{\xi}_{11}} = \frac{N}{2|g|\sigma^{\pi}_{t_{\rm m}}} \,, \qquad \frac{\bar{\xi}_{12}}{\bar{\xi}_{22}} = -\frac{N}{2|g|\sigma^{K}_{t_{\rm m}}} \,. \tag{2.47}$$

For definiteness, we take

$$\bar{\xi}_{11} = 1 \,, \qquad \bar{\xi}_{22} = \left(1 + \frac{N^2}{1-\eta^2}\right)^{-1} \,, \tag{2.48}$$

which ensures that

$$\det\xi(t) = \left(\frac{t_{\rm m}-t}{t_{\rm m}}\right)^{x} \,, \tag{2.49}$$

and thus, by the results of the previous section, would preserve the form (2.15) of the determinant of the Omnès function if $\det a(t) = 1$. The condition (2.45) on $a(t)$ requires

$$a_{21} = a_{12}\frac{\sigma^{\pi}_t}{\sigma^K_t} \,, \qquad a_{22} = a_{11} - a_{12}\frac{\eta\sin(2\delta-\psi)}{|g|\sigma^K_t} \,, \tag{2.50}$$

while a_{11} and a_{12} can be chosen freely.

Finally, $\Omega(t)$ should fulfill the normalization $\Omega(0) = \mathbb{1}$, which can be achieved by modifying the normalization in the calculation of $\Omega^\infty(t)$ appropriately. Assuming $a(0) = \mathbb{1}$, the corresponding condition

$$\Omega^\infty(0)\xi(0) = \begin{pmatrix} \bar{\xi}_{11}\big(\Omega^\infty_{11}(0) + \frac{N}{2|g|\sigma^\pi_{t_\mathrm{m}}}\Omega^\infty_{12}(0)\big) & \bar{\xi}_{22}\big(\Omega^\infty_{12}(0) - \frac{N}{2|g|\sigma^K_{t_\mathrm{m}}}\Omega^\infty_{11}(0)\big) \\ \bar{\xi}_{11}\big(\Omega^\infty_{21}(0) + \frac{N}{2|g|\sigma^\pi_{t_\mathrm{m}}}\Omega^\infty_{22}(0)\big) & \bar{\xi}_{22}\big(\Omega^\infty_{22}(0) - \frac{N}{2|g|\sigma^K_{t_\mathrm{m}}}\Omega^\infty_{21}(0)\big) \end{pmatrix} = \mathbb{1} \tag{2.51}$$

leads to

$$\Omega^\infty(0) = \left(1 + \frac{N^2}{1-\eta^2}\right)^{-1} \begin{pmatrix} \bar{\xi}^{-1}_{11} & \bar{\xi}^{-1}_{11}\frac{N}{2|g|\sigma^K_{t_\mathrm{m}}} \\ -\bar{\xi}^{-1}_{22}\frac{N}{2|g|\sigma^\pi_{t_\mathrm{m}}} & \bar{\xi}^{-1}_{22} \end{pmatrix} . \tag{2.52}$$

The above construction (2.44) ensures that $\Omega_{ij}(t)$ has the expected behavior for $t \to t_\mathrm{m}$, that the factors of $(1 - t/t_\mathrm{m})^{x_{ij}}$ factorize in (2.46) (which have therefore already been canceled there), and that $\det \bar{\Omega}(t)$ is continuous at t_m. However, in general, $\bar{\Omega}_{ij}(t)$ itself will not be continuous at t_m and the condition (2.30) will be violated.

In order to remove these shortcomings we make use of the freedom in choosing $a(t)$. In fact, a particular choice of $a(t)$ can enforce continuity of either $\bar{\boldsymbol{\Omega}}_1(t)$ or $\bar{\boldsymbol{\Omega}}_2(t)$, but not of both simultaneously. This impediment can be circumvented by noting that (2.44) may be regarded as separate equations for $\bar{\boldsymbol{\Omega}}_1(t)$ and $\bar{\boldsymbol{\Omega}}_2(t)$. We can thus derive an $\bar{\boldsymbol{\Omega}}^{(1)}_1(t)$ from a construction with an $a_1(t)$ tailored for this component (discarding $\bar{\boldsymbol{\Omega}}^{(1)}_2(t)$ in this case), $\bar{\boldsymbol{\Omega}}^{(2)}_2(t)$ from a different $a_2(t)$ (discarding $\bar{\boldsymbol{\Omega}}^{(2)}_1(t)$), and finally join these two vectors into the final Omnès matrix $\Omega(t) = \big\{\bar{\boldsymbol{\Omega}}^{(1)}_1(t), \bar{\boldsymbol{\Omega}}^{(2)}_2(t)\big\}$.

Below the two-kaon threshold we take $a_1(t) = a_2(t) = \mathbb{1}$, while for $t \geq t_K$

$$\begin{aligned} a_1(t) &= \begin{pmatrix} 1 & \frac{N(t)}{2|g(t)|\sigma^\pi_t}f(t) \\ \frac{N(t)}{2|g(t)|\sigma^K_t}f(t) & 1 - f(t) + \frac{N^2(t)}{1-\eta^2(t)}f(t) \end{pmatrix} , \\ a_2(t) &= \begin{pmatrix} 1 & -\frac{2|g(t)|\sigma^K_t}{N(t)}f(t) \\ -\frac{2|g(t)|\sigma^\pi_t}{N(t)}f(t) & 1 - f(t) + \frac{1-\eta^2(t)}{N^2(t)}f(t) \end{pmatrix} , \end{aligned} \tag{2.53}$$

with

$$N(t) = \sqrt{1 - \eta(t)^2\cos^2(2\delta(t) - \psi(t))} - \eta(t)\sin(2\delta(t) - \psi(t)) , \tag{2.54}$$

cf. (2.30), and a function $f(t)$ fulfilling $f(t_K) = 0$, $f(t_\mathrm{m}) = 1$, proves adequate. This construction makes sure that $\bar{\Omega}_{ij}(t)$ is continuous at t_m and that the relations (2.30) hold.

As we have seen in the previous section, the Omnès function is not unique, and therefore there is a priori no reason why the determinant of the resulting $\Omega(t)$ should match the single-channel expectation: we can always multiply $\bar{\boldsymbol{\Omega}}_i(t)$ with a real function $g(t)$ with $g(0) = 1$ without vitiating the above construction. Since the unitarity condition in its form analogous to (2.35) alone implies that

$$\det\Omega = \frac{2e^{i\psi}}{\eta\cos(2\delta - \psi) + \cos\psi}\big(\mathrm{Re}\,\Omega_{11}\mathrm{Re}\,\Omega_{22} - \mathrm{Re}\,\Omega_{12}\mathrm{Re}\,\Omega_{21}\big) , \tag{2.55}$$

and thus ensures the correct phase, this could be used to make the modulus of the determinant coincide with (2.15). We simply take

$$f(t) = \left(\frac{t - t_K}{t_{\rm m} - t_K}\right)^6 . \tag{2.56}$$

This choice of the exponent ensures that $f(t)$ decreases rapidly below $t_{\rm m}$, but not so fast as to cause numerical problems in the matching-point region. In this way, the single-channel result for the determinant is accurately reproduced except for the energy region close to $t_{\rm m}$.

3 Application to pion-nucleon and kaon-nucleon scattering

The $\pi\pi \to \bar{N}N$ and $\bar{K}K \to \bar{N}N$ S-waves $f_+^0(t)$ and $h_+^0(t)$, respectively, fulfill the unitarity relations (cf. [1] and appendix B)

$$\begin{aligned}
\operatorname{Im} f_+^0(t) &= \sigma_t^\pi \big(t_0^0(t)\big)^* f_+^0(t)\,\theta\big(t - t_\pi\big) + \frac{2}{\sqrt{3}}\,\sigma_t^K \big(g_0^0(t)\big)^* h_+^0(t)\,\theta\big(t - t_K\big) \;, \\
\operatorname{Im} h_+^0(t) &= \sigma_t^K \big(r_0^0(t)\big)^* h_+^0(t)\,\theta\big(t - t_K\big) + \frac{\sqrt{3}}{2}\,\sigma_t^\pi \big(g_0^0(t)\big)^* f_+^0(t)\,\theta\big(t - t_\pi\big) \;,
\end{aligned} \tag{3.1}$$

where t_0^0, g_0^0, and r_0^0 denote the $\pi\pi$, $\pi\pi \to \bar{K}K$, and $\bar{K}K$ S-waves with t-channel isospin $I_t = 0$. Since by virtue of unitarity in the $\pi\pi/\bar{K}K$ system we may identify

$$t_0^0(t) = \frac{\eta(t)e^{2i\delta(t)} - 1}{2i\sigma_t^\pi} \;, \qquad g_0^0(t) = |g(t)|e^{i\psi(t)} \;, \qquad r_0^0(t) = \frac{\eta(t)e^{2i(\psi(t)-\delta(t))} - 1}{2i\sigma_t^K} \;, \tag{3.2}$$

the unitarity relation (3.1) reduces to

$$\operatorname{Im} \mathbf{f}(t) = T^*(t)\Sigma(t)\mathbf{f}(t) \;, \qquad \mathbf{f}(t) = \begin{pmatrix} f_+^0(t) \\ \frac{2}{\sqrt{3}} h_+^0(t) \end{pmatrix} \;, \tag{3.3}$$

and with RS equations providing a dispersion relation of the form

$$\mathbf{f}(t) = \mathbf{\Delta}(t) + (\mathbf{a} + \mathbf{b}t)(t - t_N) + \frac{t^2(t - t_N)}{\pi} \int_{t_\pi}^{\infty} \mathrm{d}t' \frac{\operatorname{Im} \mathbf{f}(t')}{t'^2(t' - t_N)(t' - t)} \;, \tag{3.4}$$

where $t_N = 4m^2$, the discussion in section 2 applies. We consider here only the twice-subtracted version of the RS equations for πN scattering derived in [1]. The corresponding inhomogeneity for the πN system reads

$$\begin{aligned}
\Delta_1(t) &= \tilde{\Delta}_+^0(t) = \hat{N}_+^0(t) + \bar{\Delta}_+^0(t) \;, \\
\bar{\Delta}_+^0(t) &= \frac{1}{\pi} \int_{W_+}^{\infty} \mathrm{d}W' \sum_{l=0}^{\infty} \Big\{ \tilde{G}_{0l}\Big|^{\text{2-sub}}(t, W') \operatorname{Im} f_{l+}^+(W') + \tilde{G}_{0l}\Big|^{\text{2-sub}}(t, -W') \operatorname{Im} f_{(l+1)-}^+(W') \Big\} \,.
\end{aligned} \tag{3.5}$$

Here, $\hat{N}_+^0(t)$ denotes the nucleon pole term, $f_{l\pm}^I(W)$ the s-channel partial waves with total angular momentum $j = |l \pm 1/2|$ and isospin index $I = \pm$, and $W_+ = m + M_\pi$. Moreover, we have already neglected the contributions from higher t-channel partial waves, which were shown to be insignificant in [1]. In fact, the corresponding equation for $\Delta_2(t)$ is very similar, as long as we restrict ourselves to combinations of isospin and angular momentum that couple to $\pi\pi$ (cf. appendix B): the nucleon pole terms need to be replaced by the hyperon-pole contributions (B.10), M_π by M_K, and the Clebsch-Gordan coefficients in the relation between the s-channel amplitudes in $I=\pm$ and $I_s=0,1$ bases are different from πN (where $I_s=1/2,3/2$). In particular, the kernel functions $\tilde{G}_{0l}(t,W)$ require no further modification besides $M_\pi\to M_K$. Finally, the subtraction constants a_1 and b_1 can be related to standard πN subthreshold parameters

$$a_1=-\frac{1}{16\pi}\left(\frac{g^2}{m}+d_{00}^++b_{00}^+\frac{M_\pi^2}{3}\right), \qquad b_1=-\frac{1}{16\pi}\left(d_{01}^+-\frac{b_{00}^+}{12}\right) \tag{3.6}$$

(see [1] for precise definitions), and similarly for a_2, b_2, and KN subthreshold parameters.

Starting from the dispersion relation (3.4), the solution for $\mathbf{f}(t)$ can be derived along the lines that led to (2.12). In addition, we may use the spectral representation of the inverse of the Omnès matrix

$$\Omega^{-1}(t)=\mathbb{1}+\frac{t}{\pi}\int_{t_\pi}^{t_\mathrm{m}}\mathrm{d}t'\frac{\operatorname{Im}\Omega^{-1}(t')}{t'(t'-t)}=\mathbb{1}-t\,\dot{\Omega}(0)+\frac{t^2}{\pi}\int_{t_\pi}^{t_\mathrm{m}}\mathrm{d}t'\frac{\operatorname{Im}\Omega^{-1}(t')}{t'^2(t'-t)} \tag{3.7}$$

to perform the integrals involving $\mathbf{a}$ and $\mathbf{b}$ explicitly ($\dot{\Omega}$ denotes the derivative with respect to t). In this way, we arrive at

$$\begin{aligned}\mathbf{f}(t)&=\mathbf{\Delta}(t)+(t-t_N)\Omega(t)(\mathbb{1}-t\,\dot{\Omega}(0))\mathbf{a}+t(t-t_N)\Omega(t)\mathbf{b}\\&\quad-\frac{t^2(t-t_N)}{\pi}\Omega(t)\int_{t_\pi}^{t_\mathrm{m}}\mathrm{d}t'\frac{\operatorname{Im}\Omega^{-1}(t')\mathbf{\Delta}(t')}{t'^2(t'-t_N)(t'-t)}+\frac{t^2(t-t_N)}{\pi}\Omega(t)\int_{t_\mathrm{m}}^{\infty}\mathrm{d}t'\frac{\Omega^{-1}(t')\operatorname{Im}\mathbf{f}(t')}{t'^2(t'-t_N)(t'-t)}\,.\end{aligned} \tag{3.8}$$

To obtain the corresponding numerical results for $f_+^0(t)$ and $h_+^0(t)$ we now collect the various input needed for the explicit evaluation of (3.8). We take the $\pi\pi$ phase and inelasticity from the extended Roy-equation analysis of [21, 22] and the $\pi\pi\to\bar{K}K$ partial wave from [19], where, in the pseudophysical region $t_\pi\leq t\leq t_K$, the modulus $|g(t)|$ was determined as the solution of RS equations for πK scattering, while above the two-kaon threshold phase-shift solutions [23, 24] were used.[4] The two-channel approximation in terms of $\pi\pi$ and $\bar{K}K$ intermediate states should work well at lower energies where the $f_0(980)$ resonance dominates, but will break down once inelasticities arising from 4π intermediate states become important, which are expected to set in around $\sqrt{t_0}=1.3\,\mathrm{GeV}$. Evidently, this still leaves a large part of the $\pi\pi\to\bar{N}N$ pseudophysical region $t_\pi\leq t\leq t_N$ where intermediate states besides those considered here may contribute significantly to the spectral function. However, two subtractions should already appreciably suppress the sensitivity to this high-energy regime, which we will examine in more detail below.

[4] We are indebted to Bachir Moussallam for providing a version of the solution for $g(t)$ consistent with the $\pi\pi$ phase shift of [21, 22].

In view of the remaining uncertainties in the pseudophysical region we refrain from including information on $f_+^0(t)$ even above t_N from a phase-shift solution [25], but just put $\operatorname{Im}\mathbf{f} = 0$ above t_m. Due to continuity of the MO solution at t_m this implies that the solutions for $f_+^0(t)$ and $h_+^0(t)$ will vanish at t_m as well (unless the phases happen to pass an integer multiple of π at t_m). We take advantage of the fact that for kinematic reasons $f_+^0(t)$ and $h_+^0(t)$ have a zero at the physical threshold t_N and choose the matching point accordingly as $t_\mathrm{m} = t_N$, which should allow for a reasonably smooth matching.

Next, to evaluate the inhomogeneities $\Delta_i(t)$ we need the imaginary parts for the s-channel partial waves of πN and KN scattering. As discussed in [1], we rely on the GWU solution [26, 27] for $W \leq W_\mathrm{a} = 2.5\,\mathrm{GeV}$ in the πN case, summing up all partial waves up to $l_\mathrm{max} = 4$, and on the Regge model [28] for $W > W_\mathrm{a}$. Similarly, Δ_2 is evaluated based on [27, 29], integrating the partial waves with $l \leq 4$ up to $2\,\mathrm{GeV}$.

In the remainder of the paper we will consider three variants of the input described above. First, we take δ and ψ to be constant above t_0 ("RS1"), second, we guide δ and ψ smoothly to 2π above t_0 by means of [15]

$$\delta(t) = 2\pi + (\delta(t_0) - 2\pi)\hat{f}\Big(\frac{t}{t_0}\Big)\,, \qquad \hat{f}(x) = \frac{2}{1 + x^{3/2}}\,, \tag{3.9}$$

keeping the phase constant above t_m ("RS2"), and third, we modify RS1 in such a way that $\Delta_2 = 0$ ("RS3"). In all three cases, $|g(t)|$ is led smoothly to zero above t_m by a prescription similar to (3.9). The choice of these variants is motivated as follows. As indicated above, the model for the $\pi\pi/\bar{K}K$ S-matrix is only meaningful roughly up to t_0, and ideally our results should be insensitive to variations of this input above t_0, the simplest choice of course being to keep the phases constant. However, to ensure the correct asymptotic behavior for the scalar meson form factors, the phase ψ must tend to an asymptotic value of 2π [15], which, phenomenologically, also suggests to guide δ to 2π. Thus, RS1 and RS2 are convenient choices to assess the sensitivity to the high-energy input for the phase shifts. The results for the Omnès matrix corresponding to these two scenarios are depicted in figure 1. In addition, we compare the results for $\det\Omega(t)/(1-t/t_\mathrm{m})^x$ to the analytically known results in figure 2. As expected, the only deviations occur in the proximity of t_m, where the modifications originating from $f(t)$ according to (2.56) set in. Note that the difference between RS1 and RS2 appears slightly exaggerated here, since x differing in both cases leads to a different factor being divided out.

Finally, we use the reference point [8]

$$\frac{g^2}{4\pi} = 14.28\,, \qquad d_{00}^+ = -1.46\,M_\pi^{-1}\,, \qquad d_{01}^+ = 1.14\,M_\pi^{-3}\,, \qquad b_{00}^+ = -3.54\,M_\pi^{-3}\,, \tag{3.10}$$

although we will display the dependence of Δ_σ on each of these parameters explicitly in the end. In contrast, we are not aware of reliable input for the KN subthreshold parameters, and simply put $a_2 = b_2 = 0$. In fact, this approximation gives reason to investigate RS3, since the results from the πN sector show that the contributions from the corresponding parameters will certainly not be larger than the sum of KN Born terms (conventions for masses and couplings of the hyperons are given in appendix B) and s-channel integrals.

JHEP06(2012)063

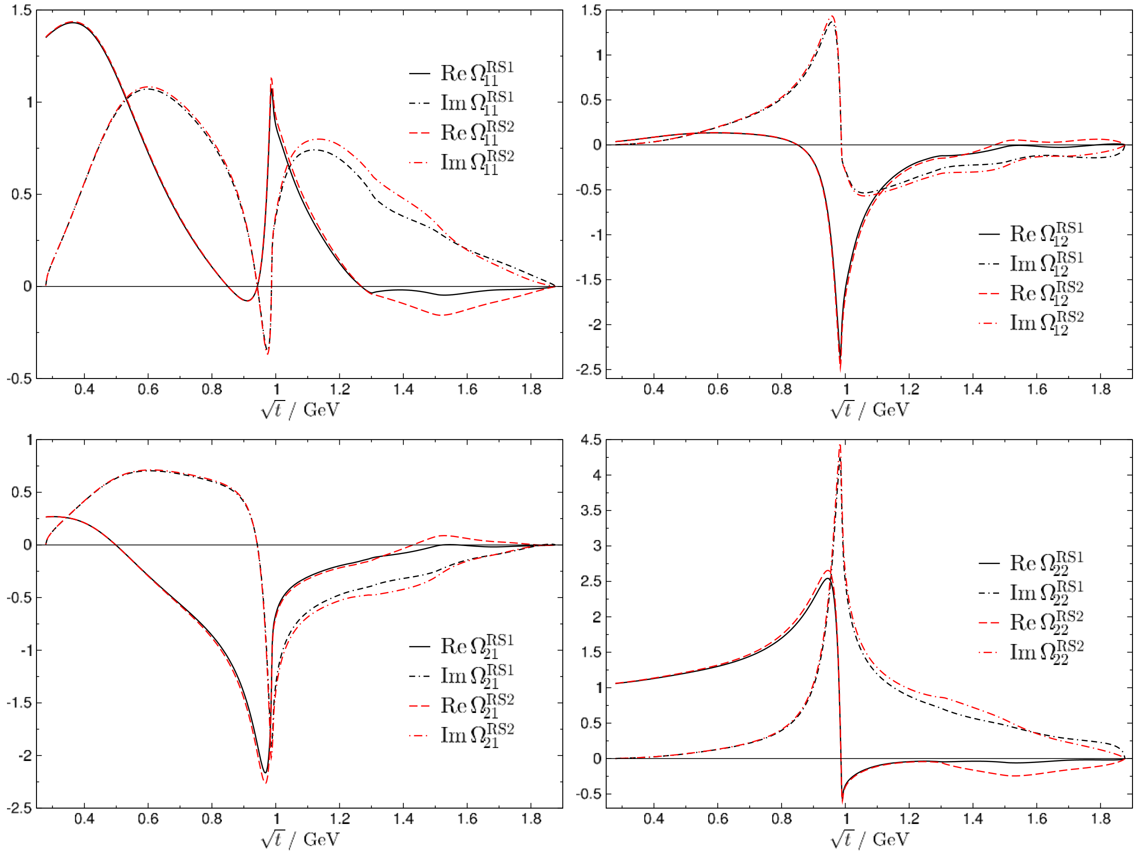

Figure 1. Results for real and imaginary part of the components of the Omnès matrix for the input phases RS1 and RS2 as described in the main text.

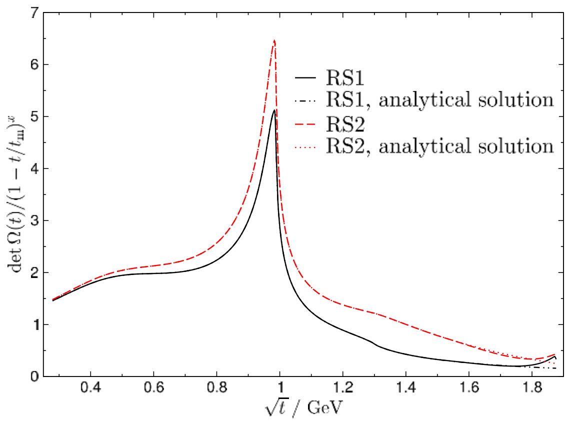

Figure 2. Comparison between numerical and analytical result for the determinant of the Omnès matrix.

The difference between RS1 and RS3 thus serves as an estimate of the uncertainty induced by neglecting the KN subthreshold parameters.

The results for $f_+^0(t)$ and $h_+^0(t)$ are shown in figure 3. In the case of $f_+^0(t)$ the agreement between the different parameter sets is very good up to 1 GeV. It is striking that the

JHEP06(2012)063

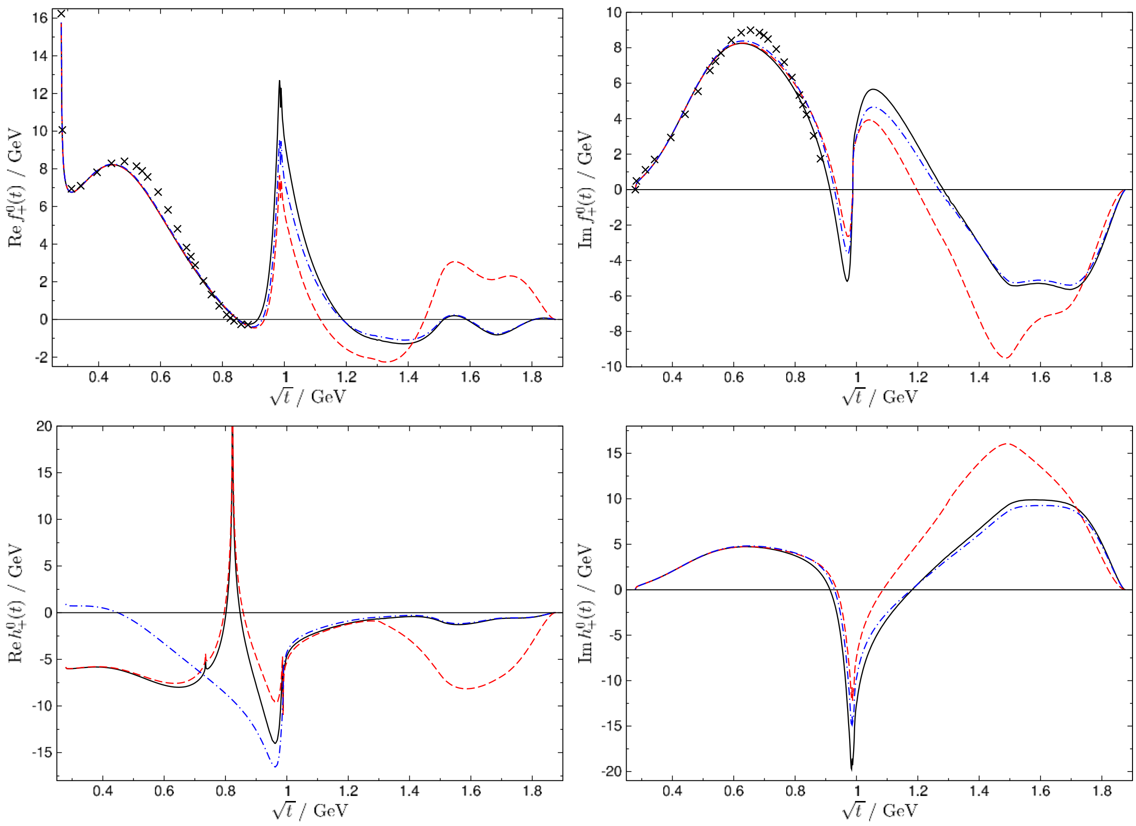

Figure 3. Results for real and imaginary part of $f_+^0(t)$ and $h_+^0(t)$. The solid, dashed, and dot-dashed lines refer to the input RS1, RS2, and RS3 as described in the main text. For $f_+^0(t)$ the black crosses indicate the results of [8].

difference between RS1 and RS2 is much larger than between RS1 and RS3, which indicates that the results are much more sensitive to the choice of the phases beyond t_0 than to the details of the KN amplitude. The real part of $h_+^0(t)$ exhibits two distinct divergences below 1 GeV that correspond to the pole-term contributions from the Λ (large peak at 0.82 GeV) and Σ (small peak at 0.73 GeV) hyperon, strictly analogous to the nucleon pole in $f_+^0(t)$ that emerges slightly below t_π. These poles, which disappear in RS3 by construction, do not pose a problem in practice, since $h_+^0(t)$ only contributes to the spectral function of the scalar form factor of the nucleon above t_K. Apart from these poles below the two-kaon threshold the conclusion is very similar to $f_+^0(t)$: the uncertainty in the phase shifts outweighs the uncertainty in the KN input.

4 Scalar form factors

4.1 Scalar pion and kaon form factors

We define the scalar pion and kaon form factors as

$$F_\pi^S(t) = \langle \pi(p')|\hat{m}(\bar{u}u + \bar{d}d)|\pi(p)\rangle\,, \quad F_K^S(t) = \langle K(p')|\hat{m}(\bar{u}u + \bar{d}d)|K(p)\rangle\,, \quad t = (p'-p)^2\,. \tag{4.1}$$

JHEP06(2012)063

In the two-channel approximation they fulfill the unitarity relation [7]

$$\operatorname{Im}\mathbf{F}^S(t) = T^*(t)\Sigma(t)\mathbf{F}^S(t)\,, \qquad \mathbf{F}^S(t) = \begin{pmatrix} F_\pi^S(t) \\ \frac{2}{\sqrt{3}}F_K^S(t) \end{pmatrix}\,, \tag{4.2}$$

and thus

$$\mathbf{F}^S(t) = \alpha\mathbf{\Omega}_1^\infty + \beta\mathbf{\Omega}_2^\infty\,, \tag{4.3}$$

with the infinite-matching-point Omnès solutions $\mathbf{\Omega}_i^\infty$ defined in (2.36). The phases δ and ψ are guided smoothly to their assumed asymptotic value of 2π according to (3.9). Using the normalization $\Omega^\infty(0) = \mathbb{1}$ of the Omnès matrix to pin down the coefficients α, β, we find

$$\begin{aligned} F_\pi^S(t) &= F_\pi^S(0)\Omega_{11}^\infty(t) + \frac{2}{\sqrt{3}}F_K^S(0)\Omega_{12}^\infty(t)\,, \\ F_K^S(t) &= \frac{\sqrt{3}}{2}F_\pi^S(0)\Omega_{21}^\infty(t) + F_K^S(0)\Omega_{22}^\infty(t)\,. \end{aligned} \tag{4.4}$$

The form factors at $t = 0$ can be determined via the Feynman-Hellmann theorem [30, 31]

$$F_\pi^S(0) = \hat{m}\frac{\partial}{\partial\hat{m}}M_\pi^2\,, \qquad F_K^S(0) = \hat{m}\frac{\partial}{\partial\hat{m}}M_K^2\,, \tag{4.5}$$

from the quark-mass dependence of the meson masses. For the pion form factor the result at $\mathcal{O}(p^4)$ in the chiral expansion reads [32]

$$F_\pi^S(0) = M_\pi^2 - \frac{M_\pi^4}{32\pi^2F_\pi^2}(\bar{l}_3 - 1) = (0.984 \pm 0.006)M_\pi^2\,, \tag{4.6}$$

where we have used $\bar{l}_3 = 3.2 \pm 0.8$ [33]. The leading-order result for the kaon form factor

$$F_K^S(0) = \frac{M_\pi^2}{2} \tag{4.7}$$

is subject to potentially large SU(3) corrections, which in the isospin limit amount to [34]

$$\begin{aligned} F_K^S(0) = \frac{M_\pi^2}{2}\Bigg\{ & 1 + \frac{M_\eta^2}{32\pi^2F_\pi^2}\log\frac{M_\eta^2}{\mu^2} + \frac{M_K^2}{72\pi^2F_\pi^2}\left(\log\frac{M_\eta^2}{\mu^2} + 1\right) - \frac{M_\pi^2}{32\pi^2F_\pi^2}\log\frac{M_\pi^2}{\mu^2} \\ & + \frac{8(2M_K^2 - M_\pi^2)}{F_\pi^2}(2L_8^{\mathrm{r}} - L_5^{\mathrm{r}}) + \frac{32M_K^2}{F_\pi^2}(2L_6^{\mathrm{r}} - L_4^{\mathrm{r}})\Bigg\}\,, \end{aligned} \tag{4.8}$$

where M_η is the mass of the η, F_π the pion decay constant, and μ the renormalization scale. Varying the low-energy constants in the range [33]

$$2L_8^{\mathrm{r}} - L_5^{\mathrm{r}} = (-0.35\ldots+0.1)\cdot 10^{-3}\,, \qquad 2L_6^{\mathrm{r}} - L_4^{\mathrm{r}} = (0\ldots+0.2)\cdot 10^{-3}\,, \tag{4.9}$$

corresponds to $F_K^S(0) = (0.4\ldots0.6)\,M_\pi^2$. In the following, we will restrict $F_K^S(0)$ to lie within these boundaries, while adopting $F_K^S(0) = M_\pi^2/2$ as our central solution.

The corresponding results for the form factors are depicted in figure 4. The phase of F_π^S coincides with δ below t_K, as required by unitarity, cf. (2.37) and (4.4). Above t_K,

JHEP06(2012)063

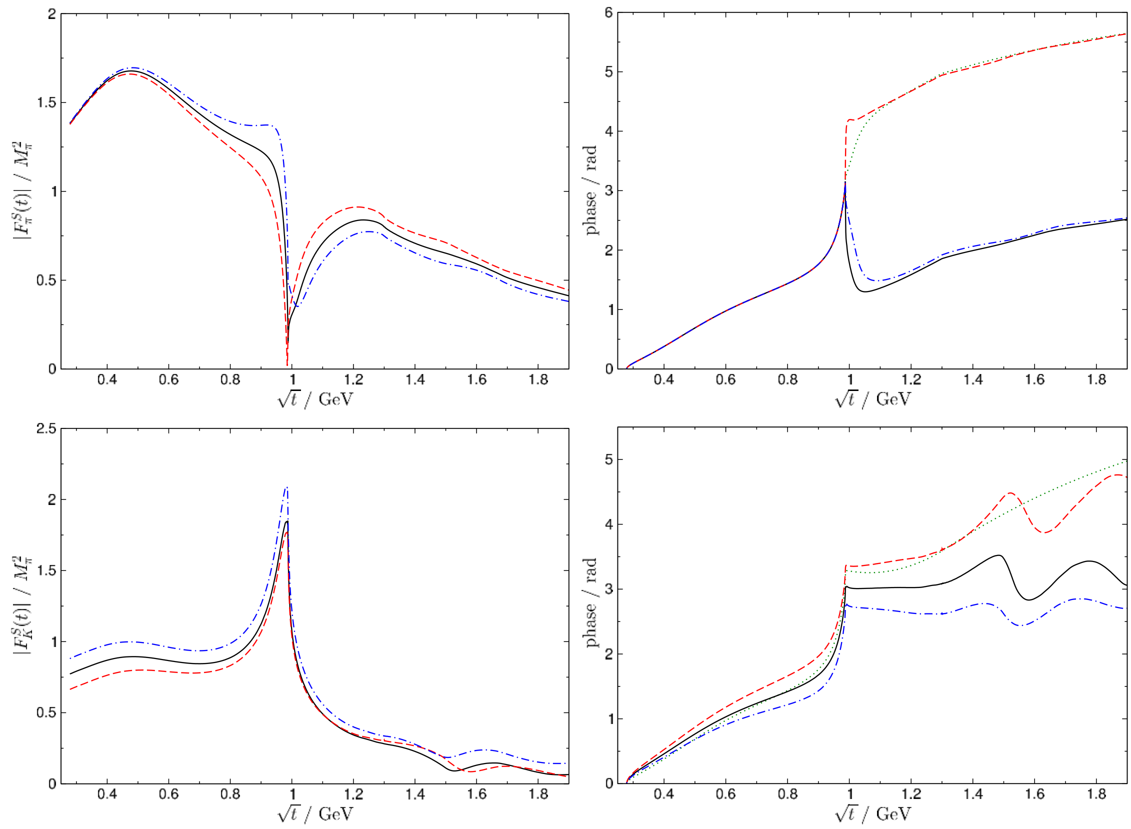

Figure 4. Modulus (left) and phase (right) of the scalar pion and kaon form factors. The solid, dashed, and dot-dashed lines refer to $F_K^S(0) = M_\pi^2/2$, $0.4\,M_\pi^2$, and $0.6\,M_\pi^2$. The phases of F_π^S and F_K^S are compared to δ and ψ, respectively, as indicated by the dotted lines.

the behavior of the phase actually depends on the assumption for $F_K^S(0)$, it either largely follows δ or abruptly drops by π. The appearance of the first scenario is surprising in view of the results of [35] (see also [36]), where only the second behavior is mentioned (the assumption for $F_K^S(0)$ agrees with our central solution). The reason for this discrepancy can be understood as follows. The S-matrix used in [35] involves a phase δ that fulfills $\delta(t_K) < \pi$. In this case, the phase δ_t of the full $\pi\pi$ partial wave t_0^0 itself displays the characteristic drop above t_K, reflecting the fact that the phase arrives at the two-kaon threshold immediately before completing a full circle in the Argand diagram. However, in recent years, it seems to have become consensus that $\delta(t_K) > \pi$ is more likely [21, 22, 37, 38], which implies that δ_t by no means exhibits a sharp drop above t_K. We conclude that the behavior of the phase cannot simply be deduced from the phase of t_0^0, it crucially depends on the relative strength $F_\pi^S(0)/F_K^S(0)$ in the superposition of the two terms involving different components of the Omnès matrix as given in (4.4), thus attesting to the inherent two-channel nature of the problem.[5] From this point of view, it is not surprising that the phase

[5]One immediate consequence is that an effective single-channel Omnès description of F_π^S in terms of the phase of F_π^S will only be applicable for certain ranges in $F_\pi^S(0)/F_K^S(0)$, unless the phase is supplemented by hand with an additional term $-\pi\theta(t - t_K)$.

$F_K^S(0)$	$0.4\,M_\pi^2$	$M_\pi^2/2$	$0.6\,M_\pi^2$
$\langle r^2\rangle_\pi^S$ [fm^2]	0.575	0.584	0.592
$\langle r^2\rangle_K^S$ [fm^2]	0.835	0.710	0.626

Table 1. Dependence of the scalar pion and kaon radii on $F_K^S(0)$.

may behave differently if $F_K^S(0)$ is varied. In contrast, the phase of $F_K^S(t)$ roughly follows the shape of ψ for all three solutions. Note that in this case (2.37) does not impose any additional constraints on the phase below t_K.

Finally, we can express the scalar radii in terms of the form factors at $t = 0$ and the derivative of the Omnès matrix

$$\langle r^2\rangle_\pi^S = 6\left\{\dot{\Omega}_{11}^\infty(0) + \frac{2}{\sqrt{3}}\frac{F_K^S(0)}{F_\pi^S(0)}\dot{\Omega}_{12}^\infty(0)\right\} ,$$
$$\langle r^2\rangle_K^S = 6\left\{\frac{\sqrt{3}}{2}\frac{F_\pi^S(0)}{F_K^S(0)}\dot{\Omega}_{21}^\infty(0) + \dot{\Omega}_{22}^\infty(0)\right\} . \tag{4.10}$$

In this way, the derivative of the Omnès matrix, e.g. for our central solution

$$\dot{\Omega}^\infty(0) = \begin{pmatrix} 2.31 & 0.32 \\ 1.26 & 0.89 \end{pmatrix} \text{GeV}^{-2} , \tag{4.11}$$

leads to the results for the scalar radii summarized in table 1. Our results for the scalar pion radius are in good agreement with $\langle r^2\rangle_\pi^S = (0.61\pm0.04)$ fm^2 from [39] and the range $\langle r^2\rangle_\pi^S = (0.583\ldots0.653)$ fm^2 found in [15]. Albeit attached with a fairly large uncertainty, the values for $\langle r^2\rangle_K^S$ lie systematically higher than its ChPT expectation $\langle r^2\rangle_K^S \sim 0.3$ fm^2 [40] (for a detailed comparison of the dispersive and the ChPT result as well as the role of $\mathcal{O}(p^6)$ corrections see [41]). In both approaches the uncertainties are substantial, either due to the large sensitivity to the specific input in the dispersive calculation or due to insufficient knowledge of low-energy constants and higher-order corrections. As the precise value of the scalar kaon radius is irrelevant for the present study, we do not consider this issue any further.

4.2 Scalar form factor of the nucleon

The scalar form factor of the nucleon is defined as

$$\sigma(t) = \frac{1}{2m}\langle N(p')|\hat{m}(\bar{u}u + \bar{d}d)|N(p)\rangle , \qquad t = (p'-p)^2 . \tag{4.12}$$

It fulfills the once-subtracted dispersion relation

$$\sigma(t) = \sigma_{\pi N} + \frac{t}{\pi}\int_{t_\pi}^{\infty} \mathrm{d}t' \frac{\operatorname{Im}\sigma(t')}{t'(t'-t)} , \tag{4.13}$$

where the pion-nucleon σ term $\sigma_{\pi N} = \sigma(0)$ acts as subtraction constant. In this way, evaluation at $t = 2M_\pi^2$ gives access to Δ_σ (as defined in (1.1)), provided that the imaginary

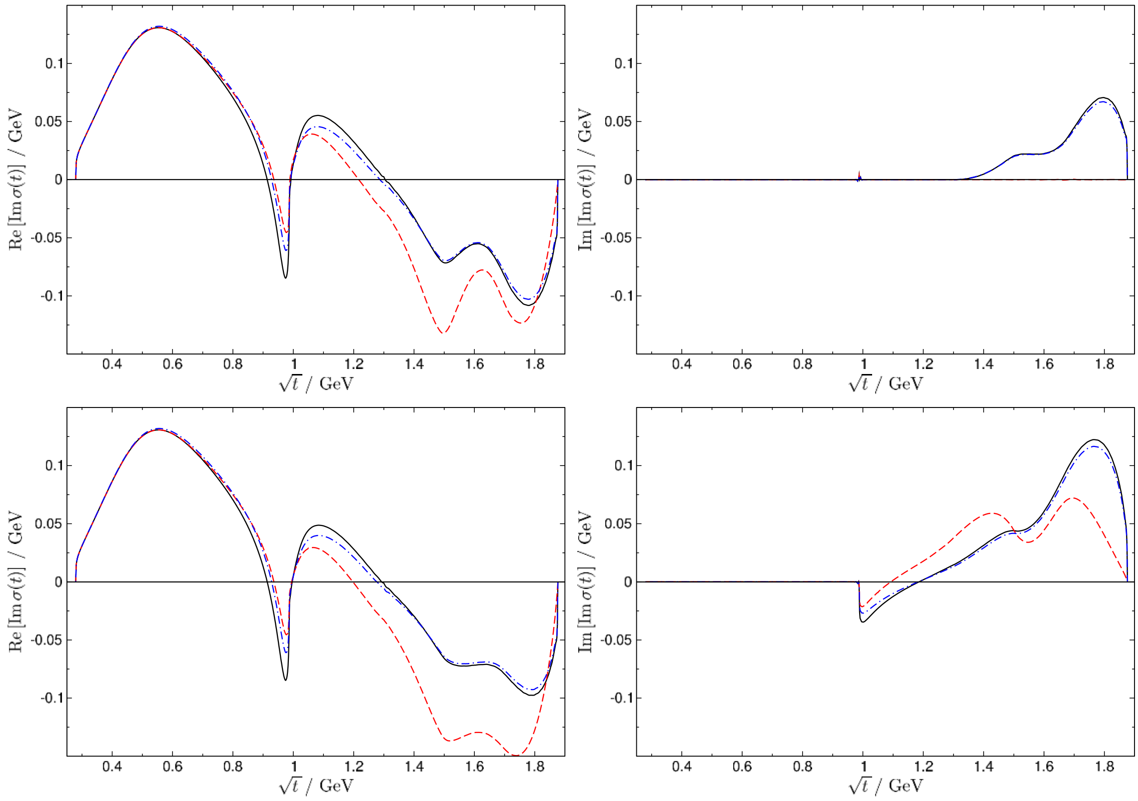

Figure 5. Real and imaginary part of $\operatorname{Im}\sigma(t)$ for our full solution (top) and with $h_+^0(t)$ set to zero (bottom). The solid, dashed, and dot-dashed lines refer to the input RS1, RS2, and RS3 as described in section 3.

part is sufficiently well constrained to perform the dispersive integral. Generalizing the result quoted in [6] by including $\bar{K}K$ intermediate states, the spectral function becomes

$$\operatorname{Im}\sigma(t) = -\frac{1}{p_t^2\sqrt{t}}\left\{\frac{3}{4}q_t\big(F_\pi^S(t)\big)^* f_+^0(t)\,\theta\big(t-t_\pi\big) + k_t\big(F_K^S(t)\big)^* h_+^0(t)\,\theta\big(t-t_K\big)\right\}. \qquad (4.14)$$

The corresponding results using the input RS1, RS2, and RS3 as discussed in section 3 as well as our central solution for the scalar pion and kaon form factors are depicted in figure 5. We also show a variant of the spectral function where the second term in the above unitarity relation (4.14) due to $\bar{K}K$ intermediate states is neglected. While the impact on the real part is moderate, we see that the spectral function develops an imaginary part starting at t_K. In contrast, our full solution stays real as long as the input for the phases is treated in the same way in the calculation of the meson-nucleon partial waves and the scalar meson form factors. For this reason, the results for RS1 and RS3 become complex around t_0, while RS2 is real in the full energy range (apart from some numerical noise at the two-kaon threshold). These findings emphasize the importance of treating inelastic channels consistently in all contributions to the unitarity relation, in particular the necessity to explicitly include the intermediate states that are responsible for the inelasticities.

The dependence of Δ_σ on the cutoff Λ of the dispersive integral is shown in figure 6. We see that the dispersion relation converges quickly and the results hardly change above

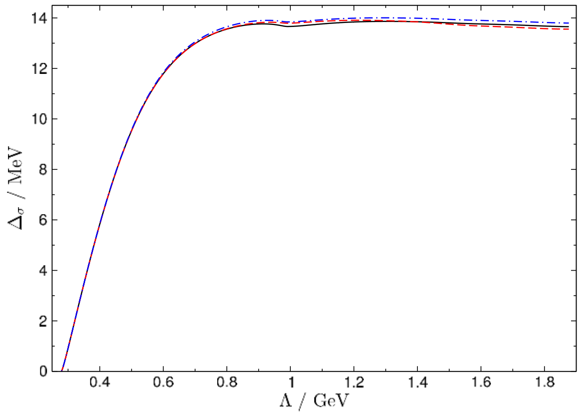

Figure 6. Δ_σ as a function of the integral cutoff Λ. Line code as in figure 5.

$(F_K^S(0),\, \Lambda)$	$(0.4\, M_\pi^2,\, 1.3\,\text{GeV})$	$(M_\pi^2/2,\, 1.3\,\text{GeV})$	$(0.6\, M_\pi^2,\, 1.3\,\text{GeV})$	$(M_\pi^2/2,\, 2m)$
RS1	13.81	13.86	13.91	13.65
RS2	13.75	13.89	14.04	13.56
RS3	13.92	14.00	14.09	13.80

Table 2. Results for Δ_σ in MeV for various combinations of $F_K^S(0)$, integral cutoff Λ, and input.

1 GeV. We quote the outcome for $\Lambda = \sqrt{t_0}$ and input RS2 as our final result, estimating the uncertainty by the variation induced by changing the cutoff to $2m$ and varying the input set or the assumption for $F_K^S(0)$ (cf. table 2). Moreover, $f_+^0(t)$ and $h_+^0(t)$ depend linearly on the πN parameters (3.10), so that the corresponding corrections for changing these parameters can be determined straightforwardly. Putting everything together, we find

$$\begin{aligned}\Delta_\sigma &= (13.9 \pm 0.3)\,\text{MeV} \\ &\quad + Z_1\left(\frac{g^2}{4\pi} - 14.28\right) + Z_2\left(d_{00}^+\, M_\pi + 1.46\right) + Z_3\left(d_{01}^+\, M_\pi^3 - 1.14\right) + Z_4\left(b_{00}^+\, M_\pi^3 + 3.54\right), \\ Z_1 &= 0.36\,\text{MeV}\,, \quad Z_2 = 0.57\,\text{MeV}\,, \quad Z_3 = 12.0\,\text{MeV}\,, \quad Z_4 = -0.81\,\text{MeV}\,. \end{aligned} \tag{4.15}$$

These results are in reasonable agreement with [6], and remarkably close to the $\mathcal{O}(p^4)$ ChPT analysis of [42] (for earlier work in ChPT on Δ_σ see [43–46])

$$\Delta_\sigma = 14.0\,\text{MeV} + 2M_\pi^4\, \bar{e}_2\,, \tag{4.16}$$

where $\bar{e}_2$ is an $\mathcal{O}(p^4)$ low-energy constant.[6] The potentially largest correction in (4.15) originates from d_{01}^+, e.g. taking $d_{01}^+ = 1.27\, M_\pi^{-3}$ from [47] increases Δ_σ by 1.6 MeV. In contrast, adjusting the coupling constant to $g^2/4\pi = 13.7$ [11, 12] only leads to a correction of -0.2 MeV. Indeed, this result is not surprising, as it is d_{01}^+ that controls the slope of the scalar form factor of the nucleon.

[6] In fact, $\bar{e}_2$ contributes to the chiral expansion of d_{01}^+.

5 Conclusion

We have presented a method to construct two-channel Omnès functions for a finite-matching-point setup, and applied this formalism to solve a coupled-channel integral equation for the $\pi\pi \to \bar{N}N$ and $\bar{K}K \to \bar{N}N$ S-waves, which can be derived from Roy-Steiner equations for πN and KN scattering. We have also repeated the conventional two-channel Muskhelishvili-Omnès calculation for the scalar pion and kaon form factors, which together with the meson-nucleon partial waves determine the spectral function of the scalar form factor of the nucleon fully including the effects of $\bar{K}K$ intermediate states. Based on these results, we have updated the dispersive analysis of the correction Δ_σ that relates the pion-nucleon σ term to the πN amplitude at the Cheng-Dashen point. Throughout the calculation we have investigated the sensitivity to various pieces of the input in detail, in particular, we give our final result for Δ_σ as a function of πN subthreshold parameters and the πN coupling constant. Our result essentially confirms the result of [6], however, using modern phase-shift input and with uncertainties due to $\bar{K}K$ effects much better under control.

Besides its implications for the scalar form factor of the nucleon, the present calculation of the $\pi\pi \to \bar{N}N$ S-wave in a full two-channel treatment completes the solution of the t-channel part of the Roy-Steiner equations derived in [1], and is also a key ingredient to pin down the πN amplitude at the Cheng-Dashen point [5, 6, 8]. Moreover, the formalism developed here should prove valuable for other systems requiring finite-matching-point two-channel Omnès solutions as well, e.g. for including $\bar{K}K$ effects into the Roy-Steiner analysis of $\gamma\gamma \to \pi\pi$ [20].

Acknowledgments

We are grateful to Bachir Moussallam for valuable discussions and to Gilberto Colangelo for providing the results of [22] prior to publication. Partial financial support by the DFG (SFB/TR 16, "Subnuclear Structure of Matter"), by the project "Study of Strongly Interacting Matter" (HadronPhysics3, Grant Agreement No. 283286) under the 7th Framework Program of the EU, by the Helmholtz Association through the Nuclear Astrophysics Virtual Institute (VH-VI-417), by the BMBF (grant 06BN9006), and by the Bonn-Cologne Graduate School of Physics and Astronomy is gratefully acknowledged.

A Continuity at the matching point

To prove the continuity of $\mathbf{f}(t)$ at t_m, we rewrite (2.12) in terms of a principal-value integral as

$$\mathbf{f}(t) = \big(\mathbb{1} + i\,T(t)\Sigma(t)\big)\boldsymbol{\Delta}(t) + \frac{\Omega(t)}{\pi}\fint_{t_\pi}^{t_\mathrm{m}} \mathrm{d}t' \frac{\Omega^{-1}(t')T(t')\Sigma(t')\boldsymbol{\Delta}(t')}{t'-t} + \frac{\Omega(t)}{\pi}\int_{t_\mathrm{m}}^{\infty} \mathrm{d}t' \frac{\Omega^{-1}(t')\mathrm{Im}\,\mathbf{f}(t')}{t'-t}\,. \tag{A.1}$$

JHEP06(2012)063

We only consider the case $t \to t_{\rm m}$ from below (continuity from above can be proven in a similar way). In this limit, the whole mass of the integral is concentrated at $t_{\rm m}$. Using (2.17), (2.18), (2.20), and (2.25), we find

$$\begin{aligned}\mathbf{f}(t_{\rm m}) = \big(\mathbb{1} + i\,T(t_{\rm m})\Sigma(t_{\rm m})\big)\boldsymbol{\Delta}(t_{\rm m}) + \frac{e^{-i\pi x}}{\det\bar\Omega(t_{\rm m})}\begin{pmatrix} I_{\rm I} & I_{\rm II} \\ I_{\rm III} & I_{\rm IV}\end{pmatrix} T(t_{\rm m})\Sigma(t_{\rm m})\boldsymbol{\Delta}(t_{\rm m}) \\ - \frac{1}{\det\bar\Omega(t_{\rm m})}\begin{pmatrix} \tilde I_{\rm I} & \tilde I_{\rm II} \\ \tilde I_{\rm III} & \tilde I_{\rm IV}\end{pmatrix}\operatorname{Im}\mathbf{f}(t_{\rm m})\,,\end{aligned} \tag{A.2}$$

with

$$\begin{aligned}
I_{\rm I} &= -\Big(\bar\Omega_{11}\bar\Omega_{22}\cot\pi x_{11} - \bar\Omega_{12}\bar\Omega_{21}\cot\pi x_{12}\Big)e^{i\psi}\,,\\
I_{\rm II} &= \bar\Omega_{11}\bar\Omega_{12}\Big(\cot\pi x_{11} - \cot\pi x_{12}\Big)e^{i\psi}\,,\\
I_{\rm III} &= -\bar\Omega_{21}\bar\Omega_{22}\Big(\cot\pi x_{11} - \cot\pi x_{12}\Big)e^{i\psi}\,,\\
I_{\rm IV} &= -\Big(\bar\Omega_{11}\bar\Omega_{22}\cot\pi x_{12} - \bar\Omega_{12}\bar\Omega_{21}\cot\pi x_{11}\Big)e^{i\psi}\,,\\
\tilde I_{\rm I} &= -\bar\Omega_{11}\bar\Omega_{22}\frac{e^{i\delta_{11}}}{\sin\pi x_{11}} + \bar\Omega_{12}\bar\Omega_{21}\frac{e^{i\delta_{12}}}{\sin\pi x_{12}}\,,\\
\tilde I_{\rm II} &= \bar\Omega_{11}\bar\Omega_{12}\left\{\frac{e^{i\delta_{11}}}{\sin\pi x_{11}} - \frac{e^{i\delta_{12}}}{\sin\pi x_{12}}\right\},\\
\tilde I_{\rm III} &= -\bar\Omega_{21}\bar\Omega_{22}\left\{\frac{e^{i\delta_{11}}}{\sin\pi x_{11}} - \frac{e^{i\delta_{12}}}{\sin\pi x_{12}}\right\},\\
\tilde I_{\rm IV} &= -\bar\Omega_{11}\bar\Omega_{22}\frac{e^{i\delta_{12}}}{\sin\pi x_{12}} + \bar\Omega_{12}\bar\Omega_{21}\frac{e^{i\delta_{11}}}{\sin\pi x_{11}}\,.
\end{aligned} \tag{A.3}$$

For the continuity condition (A.2) to be fulfilled, in particular all terms depending on $\boldsymbol{\Delta}(t_{\rm m})$ must cancel amongst themselves. Putting the coefficients of $\Delta_i(t_{\rm m})$ in each component f_i to zero yields four constraints on $I_{\rm I}$–$I_{\rm IV}$, which can be inverted to obtain

$$\begin{aligned}
I_{\rm I} &= i\det\bar\Omega\, e^{i\pi x}\frac{A - e^{2i\pi x}A^*}{A + e^{2i\pi x}A^*}\,, \qquad I_{\rm IV} = i\det\bar\Omega\, e^{i\pi x}\frac{B - e^{2i\pi x}B^*}{A + e^{2i\pi x}A^*}\,,\\
I_{\rm II} &= \frac{\sigma^K_{t_{\rm m}}}{\sigma^\pi_{t_{\rm m}}}I_{\rm III} = 4\det\bar\Omega\, e^{2i\pi x}\frac{|g|\sigma^K_{t_{\rm m}}}{A + e^{2i\pi x}A^*}\,,
\end{aligned} \tag{A.4}$$

where

$$A = \eta e^{2i\pi(x-y)} - 1\,, \qquad B = \eta e^{2i\pi y} - 1\,. \tag{A.5}$$

Similar considerations apply to $\tilde I_{\rm I}$–$\tilde I_{\rm IV}$. By means of $\operatorname{Im}\mathbf{f} = T^*\Sigma\mathbf{f}$, the remaining pieces of (A.2) can be expressed as linear combinations of f_1 and f_2, which altogether again amounts to four constraints. The solutions are

$$\begin{aligned}
\tilde I_{\rm I} &= -2i\,\det\bar\Omega\, e^{2i\pi x}\frac{A^*}{A + e^{2i\pi x}A^*}\,, \qquad \tilde I_{\rm IV} = -2i\,\det\bar\Omega\, e^{2i\pi x}\frac{B^*}{A + e^{2i\pi x}A^*}\,,\\
\tilde I_{\rm II} &= \frac{\sigma^K_{t_{\rm m}}}{\sigma^\pi_{t_{\rm m}}}\tilde I_{\rm III} = I_{\rm II}e^{-i\pi x}\,.
\end{aligned} \tag{A.6}$$

JHEP06(2012)063

Based on (2.29) it is straightforward to show that (A.4) and (A.6) hold as long as the following relations are fulfilled

$$\sqrt{1-z^2}\big(\bar\Omega_{11}\bar\Omega_{22}+\bar\Omega_{12}\bar\Omega_{21}\big)=\eta\sin\pi(2y-x)\det\bar\Omega\,,\qquad(A.7)$$
$$\sqrt{1-z^2}\bar\Omega_{11}\bar\Omega_{12}=-|g|\sigma^K_{t_\mathrm{m}}\det\bar\Omega\,,\qquad \sqrt{1-z^2}\bar\Omega_{21}\bar\Omega_{22}=|g|\sigma^\pi_{t_\mathrm{m}}\det\bar\Omega\,.$$

In this way, the properties (2.30) of the Omnès matrix finally ensure continuity at the matching point.

B Conventions for kaon-nucleon scattering

In general, we follow the notation and conventions for πN scattering of [1]. In this appendix, we briefly collect the additional formalism necessary to arrive at a closed system for πN and KN scattering.

We define the kaon states

$$|K^+\rangle=\left|\frac{1}{2},\frac{1}{2}\right\rangle\,,\quad |K^0\rangle=\left|\frac{1}{2},-\frac{1}{2}\right\rangle\,,\quad |\bar K^0\rangle=\left|\frac{1}{2},\frac{1}{2}\right\rangle\,,\quad |K^-\rangle=\left|\frac{1}{2},-\frac{1}{2}\right\rangle\,,\qquad(B.1)$$

with crossing properties

$$C|K^+\rangle=-|K^-\rangle\,,\qquad C|K^0\rangle=|\bar K^0\rangle\,,\qquad(B.2)$$

and choose the isospin decomposition of the amplitude as

$$T=T^+-\boldsymbol{\tau}_N\cdot\boldsymbol{\tau}_K T^-=T^+-2\Big(I_s(I_s+1)-\frac{3}{2}\Big)T^-\,,\qquad(B.3)$$

which leads to

$$\begin{aligned}T^{I_s=0}&=T^++3T^-\,, & T^{I_s=1}&=T^+-T^-\,,\\ T^{I_u=0}&=T^+-3T^-\,, & T^{I_u=1}&=T^++T^-\,,\\ T^{I_t=0}&=2T^+\,, & T^{I_t=1}&=2T^-\,.\end{aligned}\qquad(B.4)$$

In these equations I_s, I_t, and I_u denote s-, t-, and u-channel isospin, respectively, and $\boldsymbol{\tau}_N$ and $\boldsymbol{\tau}_K$ are the Pauli matrices associated with the nucleon and kaon isospin operators. In particular, we have

$$T^{K^\pm p}=T^{K^\pm p\to K^\pm p}=T^+\mp T^-\,.\qquad(B.5)$$

In complete analogy to πN scattering, the amplitude for the process $K(q)+N(p)\to K(q')+N(p')$ can be decomposed as

$$T^I=\bar u(p')\Big\{A^I+\frac{\not q'+\not q}{2}B^I\Big\}u(p)\,,\qquad I\in\{+,-\}\,.\qquad(B.6)$$

JHEP06(2012)063

The Born-term contributions due to hyperon pole diagrams are[7]

$$
\begin{aligned}
A^{K^+p} &= \sum_{Y=\Lambda,\Sigma} g_{KNY}^2 \frac{m_Y - m}{u - m_Y^2} , \qquad B^{K^+p} = \sum_{Y=\Lambda,\Sigma} \frac{g_{KNY}^2}{u - m_Y^2} , \\
A^{K^-p} &= \sum_{Y=\Lambda,\Sigma} g_{KNY}^2 \frac{m_Y - m}{s - m_Y^2} , \qquad B^{K^-p} = \sum_{Y=\Lambda,\Sigma} \frac{g_{KNY}^2}{s - m_Y^2} ,
\end{aligned} \tag{B.7}
$$

and hence

$$
\begin{aligned}
A^{\pm} &= \sum_{Y=\Lambda,\Sigma} g_{KNY}^2 \frac{m_Y - m}{2} \left(\frac{1}{s - m_Y^2} \pm \frac{1}{u - m_Y^2} \right) , \\
B^{\pm} &= - \sum_{Y=\Lambda,\Sigma} \frac{g_{KNY}^2}{2} \left(\frac{1}{s - m_Y^2} \mp \frac{1}{u - m_Y^2} \right) .
\end{aligned} \tag{B.8}
$$

The $\bar{K}K \to \bar{N}N$ partial waves can be obtained from the invariant amplitudes by means of the projection formula (with the t-channel scattering angle $z_t = \cos\theta_t^{KN}$)

$$
\begin{aligned}
h_+^{J,I_t=0,1}(t) &= -\frac{1}{8\pi} \int_{-1}^{1} \mathrm{d}z_t P_J(z_t) \left\{ \frac{p_t^2}{(p_t k_t)^J} A^{\pm}(t, z_t) - \frac{m}{(p_t k_t)^{J-1}} z_t B^{\pm}(t, z_t) \right\} , \\
h_-^{J,I_t=0,1}(t) &= \frac{1}{8\pi} \frac{\sqrt{J(J+1)}}{2J+1} \frac{1}{(p_t k_t)^{J-1}} \int_{-1}^{1} \mathrm{d}z_t \big(P_{J-1}(z_t) - P_{J+1}(z_t) \big) B^{\pm}(t, z_t) .
\end{aligned} \tag{B.9}
$$

The main difference to the πN t-channel partial-wave projection [49] originates from the fact that due to the lack of Bose symmetry in the $\bar{K}K$ system a partial wave with given angular momentum J couples to both $I_t = 0$ and $I_t = 1$ (corresponding to $+$ and $-$ on the right-hand side of (B.9)). In the following, we are only interested in the combination where even/odd J corresponds to $I_t = 0, 1$, respectively, since only these partial waves can occur as intermediate states in $\pi\pi \to \bar{N}N$, and will therefore suppress the isospin index. In these conventions, the Born terms are given by

$$
\begin{aligned}
h_+^J(t) &= \sum_{Y=\Lambda,\Sigma} \frac{g_{KNY}^2}{8\pi} \frac{1}{(p_t k_t)^J} \left\{ \left(\frac{p_t}{k_t} (m_Y - m) + m\tilde{y} \right) Q_J(\tilde{y}) - m\delta_{J0} \right\} , \\
h_-^J(t) &= \sum_{Y=\Lambda,\Sigma} \frac{g_{KNY}^2}{8\pi} \frac{\sqrt{J(J+1)}}{2J+1} \frac{1}{(p_t k_t)^J} \big(Q_{J-1}(\tilde{y}) - Q_{J+1}(\tilde{y}) \big) ,
\end{aligned} \tag{B.10}
$$

with

$$
\tilde{y} = \frac{t - 2M_K^2 + 2(m_Y^2 - m^2)}{4 p_t k_t} . \tag{B.11}
$$

The partial waves in the partial-wave expansion of the $\bar{K}K$ scattering amplitude

$$
R^{I_t}(s,t) = 16\pi \sum_{J=0}^{\infty} (2J+1) r_J^{I_t}(t) P_J(\cos\theta_t^{\bar{K}K}) \tag{B.12}
$$

[7] We use $m_\Lambda = 1.116\,\mathrm{GeV}$, $m_\Sigma = 1.193\,\mathrm{GeV}$ [13], and $g_{KN\Lambda}^2/4\pi = 15.55$, $g_{KN\Sigma}^2/4\pi = 0.576$ [48] for the masses and couplings of the hyperons, respectively.

obey the unitarity relation

$$\begin{aligned}\operatorname{Im} r_J^{I_t}(t) &= \sigma_t^\pi \Big|(q_t k_t)^J g_J^{I_t}(t)\Big|^2 \theta\big(t-t_\pi\big) + \sigma_t^K \Big|r_J^{I_t}(t)\Big|^2 \theta\big(t-t_K\big)\\ &+ \frac{t\sigma_t^N}{8k_t^2}\frac{1}{(c_J^{KN})^2}\Big\{\Big|H_+^J(t)\Big|^2 + \Big|H_-^J(t)\Big|^2\Big\}\theta\big(t-t_N\big)\ ,\end{aligned} \tag{B.13}$$

where $g_J^{I_t}(t)$ denotes the $\pi\pi \to \bar{K}K$ partial waves, the $\bar{K}K \to \bar{N}N$ amplitudes fulfill

$$H_+^J(t) = \frac{k_t}{p_t}(p_t k_t)^J \frac{2}{\sqrt{t}} h_+^J(t)\ , \qquad H_-^J(t) = \frac{k_t}{p_t}(p_t k_t)^J h_-^J(t)\ , \tag{B.14}$$

and $c_J^{KN} = 1/2$ is an isospin factor that emerges from the conversion between the $I_t = 0, 1$ and the $I = \pm$ basis (cf. (B.4)). With the S-matrix elements

$$\big[S_J^{I_t}(t)\big]_{\bar{K}K\to\bar{K}K} = 1 + i\frac{4k_t}{\sqrt{t}} r_J^{I_t}(t)\,\theta\big(t-t_K\big)\ , \quad \big[S_\pm^J(t)\big]^{I_t}_{\bar{K}K\to\bar{N}N} = \frac{i}{c_J^{KN}}\sqrt{\frac{p_t}{k_t}}H_\pm^J(t)\,\theta\big(t-t_N\big)\ , \tag{B.15}$$

we finally obtain the unitarity relation

$$\operatorname{Im} h_\pm^J(t) = \sigma_t^K \big(r_J^{I_t}(t)\big)^* h_\pm^J(t)\,\theta\big(t-t_K\big) + \frac{c_J^{KN}}{\sqrt{2}\,c_J}\sigma_t^\pi q_t^{2J}\big(g_J^{I_t}(t)\big)^* f_\pm^J(t)\,\theta\big(t-t_\pi\big)\ , \tag{B.16}$$

with $\pi\pi \to \bar{N}N$ partial waves $f_\pm^J(t)$ and isospin factors c_J for πN scattering (see [1] for precise definitions).

References

[1] C. Ditsche, M. Hoferichter, B. Kubis and U.-G. Meißner, *Roy-Steiner equations for pion-nucleon scattering*, *JHEP* **06** (2012) 043 [arXiv:1203.4758] [INSPIRE].

[2] T. Cheng and R.F. Dashen, *Is* SU(2) × SU(2) *a better symmetry than* SU(3)*?*, *Phys. Rev. Lett.* **26** (1971) 594 [INSPIRE].

[3] L.S. Brown, W. Pardee and R. Peccei, *Adler-Weisberger theorem reexamined*, *Phys. Rev.* **D 4** (1971) 2801 [INSPIRE].

[4] V. Bernard, N. Kaiser and U.-G. Meißner, *On the analysis of the pion-nucleon sigma term: The Size of the remainder at the Cheng-Dashen point*, *Phys. Lett.* **B 389** (1996) 144 [hep-ph/9607245] [INSPIRE].

[5] T. Becher and H. Leutwyler, *Low energy analysis of* $\pi N \to \pi N$, *JHEP* **06** (2001) 017 [hep-ph/0103263] [INSPIRE].

[6] J. Gasser, H. Leutwyler and M. Sainio, *Form-factor of the sigma term*, *Phys. Lett.* **B 253** (1991) 260 [INSPIRE].

[7] J.F. Donoghue, J. Gasser and H. Leutwyler, *The decay of a light Higgs boson*, *Nucl. Phys.* **B 343** (1990) 341 [INSPIRE].

[8] G. Höhler, *Pion-Nukleon-Streuung: Methoden und Ergebnisse*, in *Landolt-Börnstein* **9b2**, H. Schopper eds., Springer Verlag, Berlin Germany (1983).

[9] J. de Swart, M. Rentmeester and R. Timmermans, *The Status of the pion-nucleon coupling constant*, *PiN Newslett.* **13** (1997) 96 [nucl-th/9802084] [INSPIRE].

[10] R. Arndt, W. Briscoe, I. Strakovsky and R. Workman, *Extended partial-wave analysis of πN scattering data*, Phys. Rev. **C 74** (2006) 045205 [nucl-th/0605082] [INSPIRE].

[11] V. Baru et al., *Precision calculation of the $\pi^- d$ scattering length and its impact on threshold πN scattering*, Phys. Lett. **B 694** (2011) 473 [arXiv:1003.4444] [INSPIRE].

[12] V. Baru et al., *Precision calculation of threshold $\pi^- d$ scattering, πN scattering lengths and the GMO sum rule*, Nucl. Phys. **A 872** (2011) 69 [arXiv:1107.5509] [INSPIRE].

[13] Particle Data Group collaboration, K. Nakamura et al., *Review of particle physics*, J. Phys. **G 37** (2010) 075021 [INSPIRE].

[14] K.M. Watson, *Some general relations between the photoproduction and scattering of π mesons*, Phys. Rev. **95** (1954) 228 [INSPIRE].

[15] B. Moussallam, *$N(f)$ dependence of the quark condensate from a chiral sum rule*, Eur. Phys. J. **C 14** (2000) 111 [hep-ph/9909292] [INSPIRE].

[16] R. Omnès, *On the solution of certain singular integral equations of quantum field theory*, Nuovo Cim. **8** (1958) 316 [INSPIRE].

[17] S. Descotes-Genon, *Effet des boucles de quarks légers sur la structure chirale du vide de QCD*, Ph.D. Thesis, Université de Paris–Sud, Paris France (2000).

[18] N.I. Muskhelishvili, *Singular Integral Equations*, Wolters-Noordhoff Publishing, Groningen The Netherlands (1953) [2nd edition, Dover Publications, New York U.S.A. (2008)].

[19] P. Büttiker, S. Descotes-Genon and B. Moussallam, *A new analysis of πK scattering from Roy and Steiner type equations*, Eur. Phys. J. **C 33** (2004) 409 [hep-ph/0310283] [INSPIRE].

[20] M. Hoferichter, D.R. Phillips and C. Schat, *Roy-Steiner equations for $\gamma\gamma \to \pi\pi$*, Eur. Phys. J. **C 71** (2011) 1743 [arXiv:1106.4147] [INSPIRE].

[21] I. Caprini, G. Colangelo and H. Leutwyler, *Regge analysis of the $\pi\pi$ scattering amplitude*, Eur. Phys. J. **C 72** (2012) 1860 [arXiv:1111.7160] [INSPIRE].

[22] I. Caprini, G. Colangelo and H. Leutwyler, in preparation.

[23] D.H. Cohen et al., *Amplitude Analysis of the K^-K^+ System Produced in the Reactions $\pi^- p \to K^-K^+ n$ and $\pi^+ n \to K^-K^+ p$ at 6 GeV/c*, Phys. Rev. **D 22** (1980) 2595 [INSPIRE].

[24] A. Etkin et al., *Amplitude Analysis of the $K^0_S K^0_S$ System Produced in the Reaction $\pi^- p \to K^0_S K^0_S n$ at 23 GeV/c*, Phys. Rev. **D 25** (1982) 1786 [INSPIRE].

[25] A. Anisovich et al., *Partial wave analysis of $\bar{p}p \to \pi^-\pi^+$, $\pi^0\pi^0$, $\eta\eta$ and $\eta\eta'$*, Nucl. Phys. **A 662** (2000) 319 [arXiv:1109.1188] [INSPIRE].

[26] R. Arndt, W. Briscoe, I. Strakovsky and R. Workman, *Partial-wave analysis and baryon spectroscopy*, Eur. Phys. J. **A 35** (2008) 311 [INSPIRE].

[27] SAID, http://gwdac.phys.gwu.edu.

[28] F. Huang, A. Sibirtsev, J. Haidenbauer, S. Krewald and U.-G. Meißner, *Backward pion-nucleon scattering*, Eur. Phys. J. **A 44** (2010) 81 [arXiv:0910.4275] [INSPIRE].

[29] J. Hyslop, R. Arndt, L. Roper and R. Workman, *Partial wave analysis of K^+-nucleon scattering*, Phys. Rev. **D 46** (1992) 961 [INSPIRE].

[30] H. Hellmann, *Einführung in die Quantenchemie*, Franz Deuticke, Leipzig Germany (1937).

[31] R. Feynman, *Forces in Molecules*, Phys. Rev. **56** (1939) 340 [INSPIRE].

[32] J. Gasser and H. Leutwyler, *Chiral Perturbation Theory to One Loop*, *Annals Phys.* **158** (1984) 142 [INSPIRE].

[33] G. Colangelo et al., *Review of lattice results concerning low energy particle physics*, *Eur. Phys. J.* **C 71** (2011) 1695 [arXiv:1011.4408] [INSPIRE].

[34] J. Gasser and H. Leutwyler, *Chiral Perturbation Theory: Expansions in the Mass of the Strange Quark*, *Nucl. Phys.* **B 250** (1985) 465 [INSPIRE].

[35] B. Ananthanarayan, I. Caprini, G. Colangelo, J. Gasser and H. Leutwyler, *Scalar form-factors of light mesons*, *Phys. Lett.* **B 602** (2004) 218 [hep-ph/0409222] [INSPIRE].

[36] J.A. Oller and L. Roca, *Scalar radius of the pion and zeros in the form factor*, *Phys. Lett.* **B 651** (2007) 139 [arXiv:0704.0039] [INSPIRE].

[37] R. García-Martín, R. Kamiński, J. Peláez, J. Ruiz de Elvira and F. Ynduráin, *The Pion-pion scattering amplitude. IV: Improved analysis with once subtracted Roy-like equations up to 1100 MeV*, *Phys. Rev.* **D 83** (2011) 074004 [arXiv:1102.2183] [INSPIRE].

[38] B. Moussallam, *Couplings of light $I = 0$ scalar mesons to simple operators in the complex plane*, *Eur. Phys. J.* **C 71** (2011) 1814 [arXiv:1110.6074] [INSPIRE].

[39] G. Colangelo, J. Gasser and H. Leutwyler, *$\pi\pi$ scattering*, *Nucl. Phys.* **B 603** (2001) 125 [hep-ph/0103088] [INSPIRE].

[40] M. Frink, B. Kubis and U.-G. Meißner, *Analysis of the pion-kaon sigma term and related topics*, *Eur. Phys. J.* **C 25** (2002) 259 [hep-ph/0203193] [INSPIRE].

[41] J. Bijnens and P. Dhonte, *Scalar form-factors in* SU(3) *chiral perturbation theory*, *JHEP* **10** (2003) 061 [hep-ph/0307044] [INSPIRE].

[42] T. Becher and H. Leutwyler, *Baryon chiral perturbation theory in manifestly Lorentz invariant form*, *Eur. Phys. J.* **C 9** (1999) 643 [hep-ph/9901384] [INSPIRE].

[43] H. Pagels and W. Pardee, *Nonanalytic behavior of the Σ term in π-N scattering*, *Phys. Rev.* **D 4** (1971) 3335 [INSPIRE].

[44] J. Gasser and H. Leutwyler, *Quark Masses*, *Phys. Rept.* **87** (1982) 77 [INSPIRE].

[45] J. Gasser, M. Sainio and A. Švarc, *Nucleons with Chiral Loops*, *Nucl. Phys.* **B 307** (1988) 779 [INSPIRE].

[46] V. Bernard, N. Kaiser and U.-G. Meißner, *Critical analysis of baryon masses and sigma terms in heavy baryon chiral perturbation theory*, *Z. Phys.* **C 60** (1993) 111 [hep-ph/9303311] [INSPIRE].

[47] R.A. Arndt, R.L. Workman, I.I. Strakovsky and M.M. Pavan, *πN elastic scattering analyses and dispersion relation constraints*, nucl-th/9807087 [INSPIRE].

[48] B. Holzenkamp, K. Holinde and J. Speth, *A meson exchange model for the hyperon nucleon interaction*, *Nucl. Phys.* **A 500** (1989) 485 [INSPIRE].

[49] W.R. Frazer and J.R. Fulco, *Partial-Wave Dispersion Relations for $\pi\pi \to N\bar{N}$*, *Phys. Rev.* **117** (1960) 1603 [INSPIRE].

JHEP06(2012)063